

# Coherent Photoproduction from Nuclei

L. Frankfurt

*School of Physics and Astronomy, Raymond and Beverly Sackler  
 Faculty of Exact Science, Tel Aviv University, Ramat Aviv 69978,  
 Tel Aviv, Israel*

M. Strikman

*Pennsylvania State University, University Park, Pennsylvania 16802  
 M. Zhalov  
 Petersburg Nuclear Physics Institute, Gatchina 188350, Russia*

29th October 2018

## Abstract

We argue that study of the cross section of coherent photo(electro) production of vector mesons off nuclear targets provides an effective method to probe the leading twist hard QCD regimes of color transparency and perturbative color opacity as well as the onset of black body limit (BBL) in the soft and hard QCD interactions. In the case of intermediate energies we use the Generalized Vector Dominance Model (GVDM) to take into account coherence effects for two distinctive limits - the soft interactions for production of  $\rho$  and  $\rho'$ -mesons and the color transparency regime for production of charmonium states. We demonstrate that GVDM describes very well  $\rho$ -meson coherent photoproduction at  $6 \leq E_\gamma \leq 10$  GeV and predict an oscillating energy dependence for the coherent charmonium production. In the limit of small  $x$  we find that hard QCD leads to onset of the perturbative color opacity even for production of very small onium states, like  $\Upsilon$ . The advantages of the process of coherent dijet photoproduction and hard diffractive processes in general for probing the onset of BBL and measuring the light-cone wave function of the photon in a hard scattering regime where decomposition over twists becomes inapplicable are explained. We apply this analysis to the study of the photon induced coherent processes in Ultra Peripheral Collisions of ions at LHC and demonstrate that the counting rates will be sufficient to study the physics of color opacity and color transparency at the energies beyond the reach of the electron-nucleon(nucleus) colliders.

## 1 INTRODUCTION

It appears that in the next decade the photon - nucleus interactions will be in the forefront of the small  $x$  QCD dynamics studies. This is due to the possibilities of the studying coherent (and for some channels incoherent) photon - nucleus interactions at energies which exceed at least by a factor of 10 the energies of electron-nucleon interactions at HERA. Such studies will be feasible at LHC within the program of the study of the Ultra Peripheral Collisions (UPC) [1, 2, 3]. This opens a challenging opportunity to get answers to a number of the fundamental questions which could be investigated in the coherent processes: how to achieve new QCD regime of strong interaction with small coupling constant, how interactions depend on the type of the projectile and how they change with an increase of the size/thickness of the target, etc. Several regimes appear possible depending on the incident energy and the target thickness. A hadronic projectile (proton, pion, etc) high-energy interactions with the nucleus rather rapidly approach the black body limit (BBL) in which the total cross section of the interaction is equal to  $2\pi R_A^2$  ( $R_A \simeq 1.2 \cdot A^{1/3}$ ). Another extreme limit is the interaction of small size projectiles (or wave packages). In this case in a wide range of high energies the system remains almost frozen during the passage through the nucleus and the regime of color transparency is reached in which the interaction of the small size projectile with a nucleus is rather weak and proportional to  $A$ . This color transparency phenomenon in hard high energy projectile-nucleus interactions has been recently observed experimentally in the exclusive production of two jets by pions in the coherent

diffraction off nuclei. At higher energies interactions of small dipole is expected to reach the regime of the perturbative color opacity. In this regime the small size projectile still couples to the gluon field of the target via the (skewed) gluon density of the target,  $G_A(x, Q^2)$ , like in the color transparency regime. However, the scattering amplitude is not  $\propto A$  due to the leading twist (LT) shadowing,  $G_A/AG_N < 1$ . The onset of gluon shadowing tames somewhat the increase of  $G_A(x, Q^2)$  between  $x \sim 10^{-2}$  and  $x \sim 10^{-4}$  and slows down the increase of the small dipole - nucleus interaction with energy. The resulting taming is not strong enough to prevent the leading twist approximation result for the total inelastic cross section from reaching and even exceeding the BBL. This violation of unitarity is an unambiguous signal that for sufficiently small  $x$  the LT approximation breaks down.

An important practical issue for the studies of the small  $x$  dynamics is whether the interactions of small dipoles with several nucleons of the target are strongly modified by the leading twist shadowing dynamics [4] or one can neglect the LT gluon shadowing, like in the model of McLerran and Venugopalan[5], and focus on the higher twist effects which are often modeled in the impact parameter space eikonal model [6]. If the leading twist shadowing was small and only higher twist effects were taming the increase of the dipole - nucleus cross section, the break down of the DGLAP approximation would occur at rather large  $x$ . The break down of DGLAP may result in onset of the BBL or taming of the cross sections at smaller values. We will argue below that the relative importance of leading and higher twist interactions could be experimentally resolved using coherent onium photoproduction.

Note also that if the LT gluon shadowing effects were small enough, the BBL for the interaction of  $q\bar{q}$  dipoles of the size  $\geq 0.3 - 0.4 \text{ fm}$  could be reached for central collisions with heavy nuclei already at  $x \geq 10^{-3}$  that is in the kinematics where  $\ln x$  effects in the evolution of the parton densities are small. In any case, whatever is the limiting behavior for the interaction of the small size dipoles with heavy nuclei, it is of major theoretical interest since it represents a new regime of interactions when the leading twist approximation and therefore the whole notion of the parton distributions becomes inapplicable for the description of hard QCD processes in the small  $x$  regime. It is worth emphasizing that on the top of providing higher parton density targets, nuclei have another important advantage as compared to the nucleon target. It is a weak dependence of the scattering amplitude on the impact parameter for a wide range of the impact parameters (in fact, one can combine light and heavy nuclei to study the dependence of the amplitudes on the nuclear thickness). On the contrary, in the nucleon case the scattering at large impact parameters is important even at very small  $x$  working to mask the change of the regime of the interactions at small impact parameters.

Theoretical studies of the limiting behavior of the small dipole - heavy nucleus cross sections did not lead so far to definitive results. It is conceivable that the QCD dynamics will stop the increase of the cross section at central impact parameters at the values significantly smaller than allowed by the BBL. In the following discussion to emphasize the qualitative difference of the new regime we will use for simplicity the extreme hypothesis that the impact factor at small impact parameters reaches the value of one corresponding to the BBL pattern of the elastic and inelastic cross sections being equal.

There exist many processes where the projectile wave function is a superposition of configurations of different sizes, leading to the fluctuations of the interaction strength. In this respect, interactions of real and virtual photons with heavy nuclei provide unique opportunities since the photon wave function contains both the hadron-like configurations (vector meson dominance) and the direct photon configurations (small  $q\bar{q}$  components, heavy quark-antiquark components). The important advantage of the photon is that at high energies the BBL is manifested in diffraction into a multitude of the hadronic final states (elastic diffraction  $\gamma \rightarrow \gamma$  is negligible) while in the hadron case only elastic diffraction survives in the BBL, and details of the dynamics responsible for this regime remain hidden. Moreover, one can *post-select* a small size or a large size initial state by selecting a particular final state, containing for example  $c\bar{c} b\bar{b}$ , or a leading light meson. Such post-selection is much easier in the photon case than in the hadron case since the distribution over the sizes of the configurations is much broader in the photon case.

Spectacular manifestations of BBL in (virtual) photon diffraction include strong enhancement of the large mass tail of the diffractive spectrum as compared to the expectations of the triple Pomeron limit, large cross section of the high  $p_t$  dijet production [7]. We emphasize that the study of the diffractive channels will allow to distinguish between two extreme scenarios: large suppression of the cross section due to the leading twist shadowing and nonlinear regime of the BBL. Investigation of the coherent diffraction in BBL would allow to perform unique measurements of various components of the light cone wave function of the photon, providing a much more detailed information than similar measurements in the regime where leading twist

dominates.

In this review we summarize our recent studies of the various regimes of the coherent photoproduction off nuclei [7, 8, 9, 10, 11, 12, 13, 14]: the onset of the BBL regime, phenomenon of color transparency and perturbative color opacity related to the leading twist nuclear gluon shadowing, and the pattern of soft QCD phenomena in the proximity to the black body limit. In addition we consider hard leading twist diffraction off nuclei in DIS. We also outline how these effects can be studied in UPC collisions and provide a comparison with the first UPC data from RHIC.

## 2 VECTOR MESON PRODUCTION OFF NUCLEI IN THE GENERALIZED VECTOR DOMINANCE MODEL AT INTERMEDIATE ENERGIES

### 2.1 Outline of the model

Our consideration of the coherent photoproduction processes of light flavor and hidden charm is based on the use of the eikonal approximation that is the Glauber model modified to take into account finite longitudinal momentum transfer [15]. The photoproduction cross section  $\sigma_{\gamma A \rightarrow \rho A}(\omega)$  is given in the Glauber model by the general expression

$$\sigma_{\gamma A \rightarrow VA}(\omega_\gamma) = \int_{-\infty}^{t_{min}} dt \frac{\pi}{k_V^2} |F_{\gamma A \rightarrow VA}(t)|^2 = \frac{\pi}{k_V^2} \int_0^\infty dt_\perp \left| \frac{ik_V}{2\pi} \int d\vec{b} e^{i\vec{q}_\perp \cdot \vec{b}} \Gamma(\vec{b}) \right|^2. \quad (1)$$

Here  $\omega_\gamma$  is the photon energy,  $k_V$  is the vector meson momentum,  $\vec{q}_\perp^2 = t_\perp = t_{min} - t$ ,  $-t_{min} = \frac{M_V^4}{4\omega_\gamma^2}$  is the longitudinal momentum transfer in the  $\gamma - V$  transition, and  $\Gamma(\vec{b})$  is the diffractive nuclear profile function. Depending on the considered vector meson production process, the Glauber approach can be combined with either the traditional vector dominance model (VDM) (for the detailed review see Ref. [16]) or with the generalized vector dominance model (GVDM) [17, 18, 19]. More properly this latter approximation should be called the Gribov-Glauber model [20] because the space-time evolution of high energy processes is different in quantum mechanical models and in quantum field theory, and therefore theoretical foundations of the high-energy model are different. In particular, in QCD in difference from quantum mechanics a high-energy projectile interacts with all nucleons at the same impact parameter almost at the same time [20]. Due to the cancellations between diagonal and nondiagonal transitions the GVDM allows to take into account the QCD effect of the suppression of interaction of spatially small quark-gluon wave packages with a hadron target - the so called color transparency phenomenon. Namely, cancellations occur between the amplitudes of the photon transition into a vector state  $V_1$  with subsequent conversion to a state  $V_2$  and direct production of the state  $V_2$ , etc. The importance of the nondiagonal transitions reveals itself in the precocious Bjorken scaling for moderately small  $x \sim 10^{-2}$  as due to the presence in the virtual photon of hadron-like and point-like type configurations [21]. These amplitudes are also crucial for ensuring a quantitative matching with perturbative QCD regime for  $Q^2 \leq$  few GeV $^2$  [22]. The amplitude of the vector meson production off a nucleon can be written within the GVDM as

$$A(\gamma + N \rightarrow V_j + N) = \sum_i \frac{e}{f_{V_i}} A(V_i + N \rightarrow V_j + N), \quad (2)$$

where  $f_{V_i}$  are expressed through  $\Gamma(V_i \rightarrow e^+ e^-)$ . Calculation of the vector meson production amplitude off nuclei within the Glauber approximation requires taking into account both the nondiagonal transitions due to the transition of the photon to a different meson  $V'$  in the vertex  $\gamma \rightarrow V'$  and due to a change of the meson in multiple rescatterings like  $\gamma \rightarrow V \rightarrow V' \rightarrow V$ . This physics is equivalent to inelastic shadowing phenomenon familiar from hadron-nucleus scattering [20]. Then in the optical limit ( $A \gg 1$ ) of the Glauber multistep production theory one can introduce the eikonal functions,  $\Phi_{V,V'}(\vec{b}, z)$ , which describe propagation of the produced objects through the medium and are related to the diffractive profile function by expression

$$\Gamma(\vec{b}) = \lim_{z \rightarrow \infty} \Phi(\vec{b}, z). \quad (3)$$

Within the optical limit of the Glauber based GVDM with accuracy  $O(\sqrt{\alpha}_{em})$  the eikonal functions  $\Phi_{V,V'}(\vec{b}, z)$  are determined by the solutions of the coupled channel equations

$$\frac{d}{dz} \sum_V \Phi_V(\vec{b}, z) = \sum_V \frac{1}{2ik_V} \left[ U_{\gamma A \rightarrow VA}(\vec{b}, z) e^{iq_{\parallel}^{\gamma \rightarrow V} z} + \sum_{V'} U_{VA \rightarrow V' A}(\vec{b}, z) e^{iq_l^{V \rightarrow V'} z} \Phi_{V'}(\vec{b}, z) \right], \quad (4)$$

with the initial condition  $\Phi_{V,V'}(\vec{b}, -\infty) = 0$ . The exponential factors  $\exp[iq_{\parallel}^{i \rightarrow j} z]$  are responsible for the coherent length effect,  $i, j = \gamma, V, V'$ ,  $q_l^{i \rightarrow j} = \frac{M_j^2 - M_i^2}{2\omega_{\gamma}}$ . The generalized Glauber -based optical potentials in the short-range approximation are given by the expression

$$U_{iA \rightarrow jA}(\vec{b}, z) = -4\pi f_{iN \rightarrow jN}(0) \varrho(\vec{b}, z). \quad (5)$$

Here  $f_{iN \rightarrow jN}(0)$  are the forward elementary amplitudes, and  $\varrho(\vec{b}, z)$  is the nuclear density normalized by the condition  $\int d\vec{b} dz \varrho(\vec{b}, z) = A$ . We calculated  $\varrho(\vec{b}, z)$  in the Hartree-Fock-Skyrme (HFS) model which provided a very good (with an accuracy  $\approx 2\%$ ) description of the global nuclear properties of spherical nuclei along the periodical table from carbon to uranium[23] and the shell momentum distributions in the high energy (p,2p)[24] and (e,e'p)[25] reactions. If the nondiagonal rescattering amplitudes  $f_{VN \rightarrow V'N} = 0$ , one can easily integrate Eq.4, and using the expression for the elementary amplitude

$$f_{VN \rightarrow VN}(t = 0) = \frac{1}{4\pi} k_V \sigma_{VN}^{tot} (1 - i\alpha_{VN}),$$

obtain the expression for the photoproduction cross section:

$$\frac{d\sigma_{\gamma A \rightarrow VA}}{dt} = \frac{d\sigma_{\gamma N \rightarrow VN}(t = 0)}{dt} \left| \int d^2 b dz e^{i\vec{q}_t \cdot \vec{b}} \rho(\vec{b}, z) e^{iq_l z} \cdot e^{-\frac{1}{2}\sigma_{VN}^{tot}(s)(1-i\alpha_{VN}) \int_z^{\infty} \rho(\vec{b}, z') dz'} \right|^2, \quad (6)$$

well known from early seventies (see for example [16]).

## 2.2 Production of light vector mesons

We have used the GVDM to describe coherent photoproduction of hadronic states of  $M \leq 2$  GeV off nuclei and consider the onset of BBL in the soft regime<sup>1</sup>. In Ref. [26] the simplest nondiagonal model was considered with two states  $\rho$  and  $\rho'$ . Then the GVDM comprises elementary amplitudes

$$\begin{aligned} f_{\gamma N \rightarrow \rho N} &= \frac{e}{f_{\rho}} f_{\rho N \rightarrow \rho N} + \frac{e}{f_{\rho'}} f_{\rho' N \rightarrow \rho N}, \\ f_{\gamma N \rightarrow \rho' N} &= \frac{e}{f_{\rho'}} f_{\rho' N \rightarrow \rho' N} + \frac{e}{f_{\rho}} f_{\rho N \rightarrow \rho' N}. \end{aligned} \quad (7)$$

It was assumed that both  $\rho$  and  $\rho'$  have the same diagonal amplitudes of scattering off a nucleon. The ratio of coupling constants was fixed:  $f_{\rho'}/f_{\rho} = \sqrt{3}$ , while the ratio of the nondiagonal and diagonal amplitudes  $A(\rho + N \rightarrow \rho' + N)/A(\rho + N \rightarrow \rho + N) = -\epsilon$ , and the value  $\sigma_{\rho N}^{tot}$  were found from the fit to the forward  $\gamma + A \rightarrow \rho + A$  cross sections measured at  $\omega_{\gamma} = 6.1, 6.6$  and  $8.8$  GeV[27]. One should emphasize here that in such GVDM extension  $\rho'$ -meson approximates the hadron production in the interval of hadron masses  $\Delta M^2 \sim 2\text{GeV}^2$ . Thus the values of the production cross section refer to the corresponding mass interval.

We refined this model in [9]. The dependence on the nuclear structure parameters was diminished by calculating the nuclear densities in the Hartree-Fock-Skyrme (HFS) approach. Next, we used in all our calculations the parameterization of [28] for the  $\rho N$  amplitude which was obtained from the fit to the experimental data on photoproduction off the proton target. The value of  $\epsilon$  was fixed at 0.18 to ensure the best fit of the measured differential cross section of the  $\rho$ -meson photoproduction off lead at  $\omega_{\gamma} = 6.2$

<sup>1</sup>In our calculation we neglect the triple Pomeron contribution which is present at high energies. This contribution though noticeable for the scattering off the lightest nuclei becomes a very small correction for the scattering of heavy nuclei due the strongly absorptive nature of the interaction at the central impact parameters.

GeV and  $t_\perp = 0.001 \text{ GeV}^2$ . Note that this value of  $\epsilon$  leads to a suppression of the differential cross section of the  $\rho$ -photoproduction in  $\gamma + p \rightarrow \rho + p$  by a factor of  $(1 - \epsilon/\sqrt{3})^2 \approx 0.80$  practically coinciding with phenomenological renormalization factor  $R = 0.84$  introduced in [28] to achieve the best fit of the elementary  $\rho$ -meson photoproduction forward cross section in the VDM which neglects mixing effects. With all parameters fixed we calculated the differential cross sections of  $\rho$ -production off nuclei and found a good agreement with the data [27], see a detailed comparison in [9]. In view of a good agreement of the model with the data on  $\rho$ -meson production in the low energy domain we used this model to consider the  $\rho$ -meson photoproduction at higher energies of photons. The increase of the coherence length with the photon energy leads to a qualitative difference in the energy dependence of the coherent vector meson production off light and heavy nuclei and to a change of the A-dependence for the ratio of the forward  $\rho'$  and  $\rho$ -meson production cross sections between  $\omega_\gamma \sim 10 \text{ GeV}$  and  $\omega_\gamma \sim 40 \text{ GeV}$  (Fig.1). The observed pattern reflects the difference of the coherence lengths of the  $\rho$ -meson and a heavier  $\rho'$ -meson which is important for the intermediate photon energies  $\leq 30 \text{ GeV}$ . The corrections due to nondiagonal transitions are relatively small ( $\sim 15\%$ ) for the case of  $\rho$  production off a nuclei. As a result, we find that the GVDM cross section is close to the one calculated in the VDM for heavy nuclei as well. Situation for  $\rho'$  production is much more interesting. The cross section of  $\rho'$  production off a nucleon is strongly suppressed as compared to the case when the  $\rho \leftrightarrow \rho'$  transitions are switched off. The extra suppression factor is  $\approx 0.5$ . The non-diagonal transitions disappear in the limit of large A (corresponding to the BBL) due to the condition of orthogonality of hadronic wave functions in accordance with the general argument of Gribov [17]. Therefore in the limit of  $A \rightarrow \infty$  we expect that the relation

$$\frac{d\sigma(\gamma + A \rightarrow h_1 + A)/dt}{d\sigma(\gamma + A \rightarrow h_2 + A)/dt}_{|A \rightarrow \infty} = \frac{\sigma(e^+ e^- \rightarrow h_1)}{\sigma(e^+ e^- \rightarrow h_2)} \approx (f_2/f_1)^2, \quad (8)$$

should be fulfilled for the productions of states  $h_1, h_2$  of invariant masses  $M_1^2, M_2^2$  at  $t_\perp = 0$ . Indeed we have found from calculations that in the case of the coherent photoproduction off lead the nondiagonal transitions becomes strongly suppressed with increase of the photon energy. As a result the  $\rho'/\rho$  ratio increases, exceeds the ratio of the  $\gamma p \rightarrow Vp$  forward cross sections calculated with accounting for  $\rho \leftrightarrow \rho'$  transitions already at  $\omega_\gamma \geq 50 \text{ GeV}$  and becomes close to the value of  $f_{\rho'}^2/f_\rho^2$  which can be considered as the limit when one can treat the interaction with the heavy nucleus as a black one. It is worth noting here that presence of nondiagonal transitions in terms of the formalism of the scattering eigen states [29] corresponds to the fluctuations of the values of the interaction cross sections for the real photon. The GVDM discussed in the paper leads to small ( $\propto 10\%$ ) color transparency effects at intermediate energies for the cross section of semiinclusive photoproduction processes. Really, this model corresponds to the propagation of states with cross sections:  $\approx \sigma(VN)(1 \pm \epsilon)$ . In the case of electroproduction  $\epsilon$  should be significantly larger:

$$\epsilon \approx \frac{f_{\rho'}}{f_\rho} = \sqrt{\frac{\Gamma(\rho \rightarrow e^+ e^-)}{m_\rho} / \frac{\Gamma(\rho' \rightarrow e^+ e^-)}{m_{\rho'}}}.$$

This equation follows from Eq.(2) where the left hand side is put to zero because the cross section of the elastic vector meson electroproduction rapidly decreases with  $Q^2$ . The presence of the CT phenomenon within the GVDM leads to a substantial modification of the pattern of the approach to BBL. The nondiagonal transitions become more important with the increase of  $Q^2$ , leading to an enhancement of the effects discussed above. In particular, the fluctuations of strengths of interaction would lead at large  $Q^2$  to the color transparency phenomenon. Presence in GVDM of significantly different masses of  $\rho, \rho', \dots$  makes it impossible to describe all fluctuations of strengths of interaction in terms of one coherent length.

### 2.3 Photoproduction of $J/\psi, \psi'$ -mesons at intermediate energies.

There is a qualitative difference between GVDM description of the light meson production described above and production of charmonium states. In the case of the photoproduction of light mesons the soft physics dominates both at low and high energies. Hence, the Gribov-Glauber model should be applicable in a wide range of energies. At the same time the space-time picture of the process changes with energy. At low energies the meson is formed at the distances smaller than the typical interaction length of a meson in the nucleus. With the increase of energy the formation length starts to exceed the nuclear size and a photon

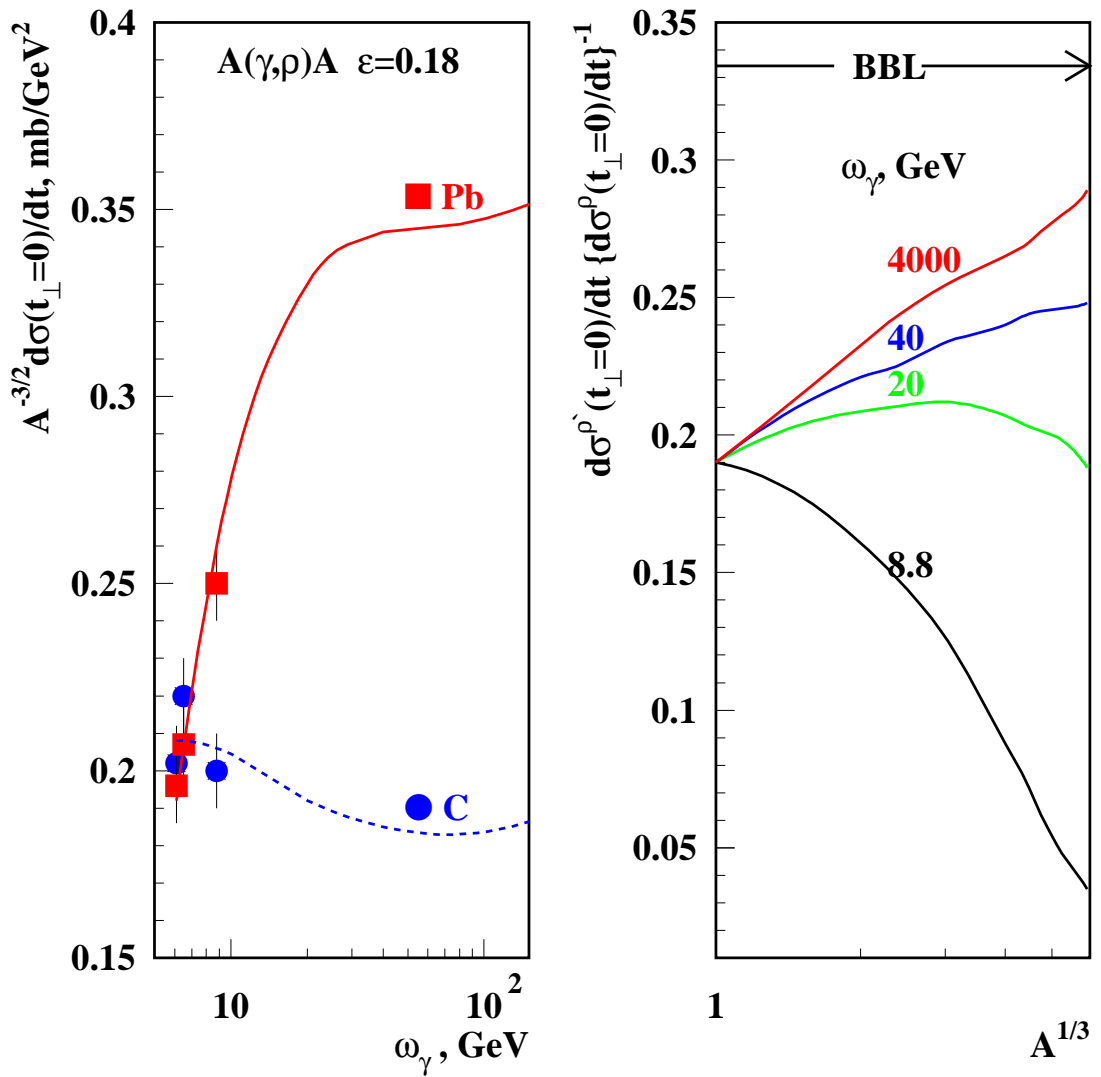


Figure 1: The energy dependence of the  $\rho$ -photoproduction cross section and the  $A$ -dependence of the  $\rho'/\rho$  photoproduction cross sections calculated in the GVDM+Glauber model.

converts to a system of  $q\bar{q}$  and higher Fock-components before the target, and one has to account for the interactions of this system with the media and subsequent transition of the system to a vector meson.

The situation is much more involved in the case of (charm)onium production. At high energies both the coherence length  $l_c \approx 2\omega_\gamma m_V^{-2}$  and the formation length  $l_f \approx 2\omega_\gamma [m_{\psi'}^2 - m_{J/\psi}^2]^{-1}$  (distance on which the squeezed  $q\bar{q}$  pair transforms into the ordinary meson) are large and the color transparency phenomenon reveals itself. In particular, it explains the fast increase of the cross section with energy observed at HERA (for reviews of small  $x$  phenomena see Ref. [30, 31]). Consequently, the value of the cross section extracted from the charmonium photoproduction characterizes the interaction of the squeezed  $c\bar{c}$  pair with a nucleon rather than the charmonium-nucleon interaction. In the high energy limit the very small interquark distances in the wave function of the photon dominate, and one has to treat the interaction of small dipoles with nuclei. In this case the eikonal approximation gives a qualitatively wrong answer since it does not take into account the leading twist effect of the gluon shadowing (see the detailed analysis in [32]), while the leading twist analysis predicts large shadowing effects [8], see discussion in section 3. On the other hand, at the intermediate energies when onium states are formed inside the nucleus the nonperturbative effects at a transverse distance scale comparable to the charmonium size becomes important. The hadronic basis description would be more relevant in this case. However the VDM which takes into account only diagonal vector meson transitions does not account properly for the basic QCD dynamics of interaction. In particular, SLAC data [33] show that  $\sigma_{\gamma+N \rightarrow \psi'N} \approx 0.15 \cdot \sigma_{\gamma+N \rightarrow \psi N}$  which within VDM corresponds to:  $\sigma_{\psi'N}/\sigma_{J/\psi N} \approx 0.7$ . This conclusion is in evident contradiction with the QCD expectation that the hadron interaction cross section should be scaled approximately as the transverse area occupied by color:  $\sigma_{\psi'N}/\sigma_{J/\psi N} \propto r_{\psi'}^2/r_{J/\psi}^2$ . Thus in this naive QCD picture  $\sigma(\psi'N)/\sigma(J/\psi N) \sim 4$ . A QCD explanation of such failure of VDM is based on the observation [34, 35] that in photoproduction of both the  $J/\psi$  and  $\psi'$  mesons the small relative distances  $\sim 1/m_c$  dominate in the  $c\bar{c}$  component of the photon wave function. Therefore the cross sections which enter into the ratio of  $J/\psi$  and  $\psi'$  yields are cross sections of the interaction of the small dipoles, not genuine mesons. The suppression of the production of  $\psi'$  in this picture is primarily due to a smaller leptonic decay width of  $\psi'$  (a factor of 1/3). A significant additional suppression comes from importance of more massive  $c\bar{c}$  intermediate states in the photon wave function ( $\geq M_{J/\psi}, M_{\psi'}$  respectively). The exact value of the suppression is sensitive to the details of the onium wave functions and the dependence of the dipole - nucleon cross section on the size of the dipole [36, 37].

The dominance of small  $c\bar{c}$  configurations in photoproduction processes is relevant for the significant probability of nondiagonal  $J/\psi \leftrightarrow \psi'$  diffractive transitions. The GVDM adjusted to account for the color screening phenomenon [34, 35] allows to take into account QCD dynamics using a hadronic basis. Such a description is limited to the regime of small coherence lengths (medium energies), where leading twist shadowing is not important. We use the GVDM to consider the coherent photoproduction of hidden charm mesons off nuclei at moderate photon energies  $20 \text{ GeV} \leq \omega_\gamma \leq 60 \text{ GeV}$  where the coherence length for the  $\gamma V$  transition  $l_c$  is still close enough to the internucleon distance in nuclei while the formation length  $l_f$  is comparable to the radii of heavy nuclei. In this energy range produced charmonium states have a noticeable probability to rescatter in sufficiently heavy nuclei. Therefore, one would be able to reveal the fluctuation of the charmonium-nucleon interaction strength as due to the diagonal  $\psi N \rightarrow \psi N$  and nondiagonal  $\psi N \leftrightarrow \psi'N$  rescatterings for moderate energies. The GVDM which we outlined above takes into account the coherence length effects via the Glauber model approximation. The key distinction from the  $\rho$ -meson case is choosing the parameters of the model to account for the space-time evolution of spatially small  $c\bar{c}$  pair. It is important that the inelastic shadowing corrections related to the production of higher mass states [20] are still insignificant. A reasonable starting approximation to evaluate the amplitude of the charmonium-nucleon interaction is to restrict ourselves to the basis of  $J/\psi$  and  $\psi'$  states for the photon wave function in Eq.2. Then, similarly to the considered above case of  $\rho, \rho'$  production we have two equations comprising six elementary amplitudes. The charmonium-nucleon coupling constants:  $\frac{f_{J/\psi}^2}{4\pi} = 10.5 \pm 0.7$ , and  $\frac{f_{\psi'}^2}{4\pi} = 30.9 \pm 2.6$  are determined from the widths of the vector meson decays  $V \rightarrow e\bar{e}$ . Since in the photoproduction processes  $c\bar{c}$  pair is produced within the spatially small configuration one can neglect for a moment by the direct photoproduction amplitude and obtain the approximative relations between rescattering amplitudes

$$f_{\psi' N \rightarrow \psi' N} \approx -\frac{f_{\psi'}}{f_{J/\psi}} f_{\psi' N \rightarrow J/\psi N} \approx \frac{f_{\psi'}^2}{f_{J/\psi}^2} f_{J/\psi N \rightarrow J/\psi N}. \quad (9)$$

Large values for nondiagonal amplitudes  $f_{\psi' N \rightarrow J/\psi N} \approx -1.7 f_{J/\psi N \rightarrow J/\psi N}$  are a characteristic QCD property of hidden charm and beauty meson-nucleon interaction. Note that the negative sign of the nondiagonal amplitude is dictated by the QCD factorization theorem. A positive sign of the forward photoproduction  $f_{\gamma N \rightarrow J/\psi(\psi') N}$  amplitudes as well as the signs of the coupling constants  $f_{J/\psi}$  and  $f_{\psi'}$  are determined by the signs of the charmonium wave functions at  $r=0$ . From the approximative estimates above it also follows that  $\sigma_{\psi' N} \approx 9\sigma_{J/\psi N}$ . This is much larger than  $\sigma_{\psi' N} \sim 20 \text{ mb}$  suggested by analyses of the data on  $\psi'$  absorption in nucleus-nucleus collisions [38, 39]. When combined with the SLAC data [40], this corresponds to  $\sigma_{\psi' N} / \sigma_{J/\psi N} \approx 5 \div 6$  with large experimental and theoretical errors.

To fix elementary amplitudes more accurately within GVDM (see [12] for details) we parameterized the elementary photoproduction cross section in the form used by the experimentalists of HERA to describe their data. This form has no firm theoretical justification but it is convenient for the fit

$$\sigma_{\gamma+N \rightarrow V+N} \propto F_{2g}^2(t) \left( \frac{s}{s_0} \right)^{0.4}. \quad (10)$$

Here  $s = 2\omega_\gamma m_N$  is the invariant energy for the photon scattering off a free nucleon,  $s_0 = 40 \text{ GeV}^2$  is the reference point and  $F_{2g}(t)$  is the two-gluon form factor of a nucleon.

We also used the SLAC results for the forward  $\gamma N \rightarrow J/\psi N$  cross section [33] and for the ratio

$$\frac{d\sigma_{\gamma N \rightarrow \psi' N}}{dt} \Big|_{t=t_{min}} = 0.15 \cdot \frac{d\sigma_{\gamma N \rightarrow J/\psi N}}{dt} \Big|_{t=t_{min}}. \quad (11)$$

Besides, we fixed the  $J/\psi N$  cross section  $\sigma_{J/\psi N} \approx (3.5 \pm 0.8) \text{ mb}$  as measured at SLAC[40] and used the reasonable assumption about the energy dependence of this cross section as the sum of soft and hard physics:

$$\sigma_{J/\psi N} = 3.2 \text{ mb} \left( \frac{s}{s_0} \right)^{0.08} + 0.3 \text{ mb} \left( \frac{s}{s_0} \right)^{0.2}. \quad (12)$$

The existence of a hard part of the  $J/\psi N$  cross section is consistent with the GVDM, because the photoproduction amplitude has a stronger energy dependence than the Pomeron exchange, i.e. soft scattering amplitudes. Next, we used this input, the optical theorem and the well known Gribov-Migdal relation

$$\Re f_{\Psi N \rightarrow \Psi N} = \frac{s\pi}{2} \frac{\partial}{\partial \ln s} \frac{\Im f_{\Psi N \rightarrow \Psi N}}{s}, \quad (13)$$

to determine from Eq.2 all elementary amplitudes in the discussed energy range. In particular, we found the value  $\sigma_{\psi' N} \approx 8 \text{ mb}$ . However, the input parameters of the GVDM, namely the experimental cross sections of the forward elementary photoproduction and, especially, the value of  $\sigma_{J/\psi N}$ , are known with large uncertainties. In result, we obtained elementary cross sections changing in the ranges:  $2.5 \text{ mb} \leq \sigma_{J/\psi N} \leq 5 \text{ mb}$  and  $6 \text{ mb} \leq \sigma_{\psi' N} \leq 12 \text{ mb}$ , in the discussed energy range. We checked how a variation of  $\sigma_{J/\psi N}$  within the experimental errors influences our results.

In our papers[12],[13] we analyzed the coherent photoproduction of charmonia off light(Si) and heavy(Pb) nuclei. Here we present the cross sections of the coherent photoproduction of  $J/\psi$  and  $\psi'$  off Ca. The energy dependence of these cross sections is compared (Fig.2a) to that obtained in the Impulse Approximation where all rescatterings of the produced vector mesons are neglected, and the cross section is given by the simple formula

$$\frac{d\sigma_{\gamma A \rightarrow VA}(s, t)}{dt} = \frac{d\sigma_{\gamma N \rightarrow VN}(s, t_{min})}{dt} \cdot \left| \int_0^\infty e^{i\vec{q}_\perp \cdot \vec{b}} d\vec{b} \int_{-\infty}^\infty dz e^{iz \cdot \vec{q}_\parallel^\gamma V} \varrho(\vec{b}, z) \right|^2. \quad (14)$$

The distinctive feature of the coherent charmonium photoproduction is that differential cross sections oscillate as a function of the photon energy. The major source for such a behavior at intermediate energies

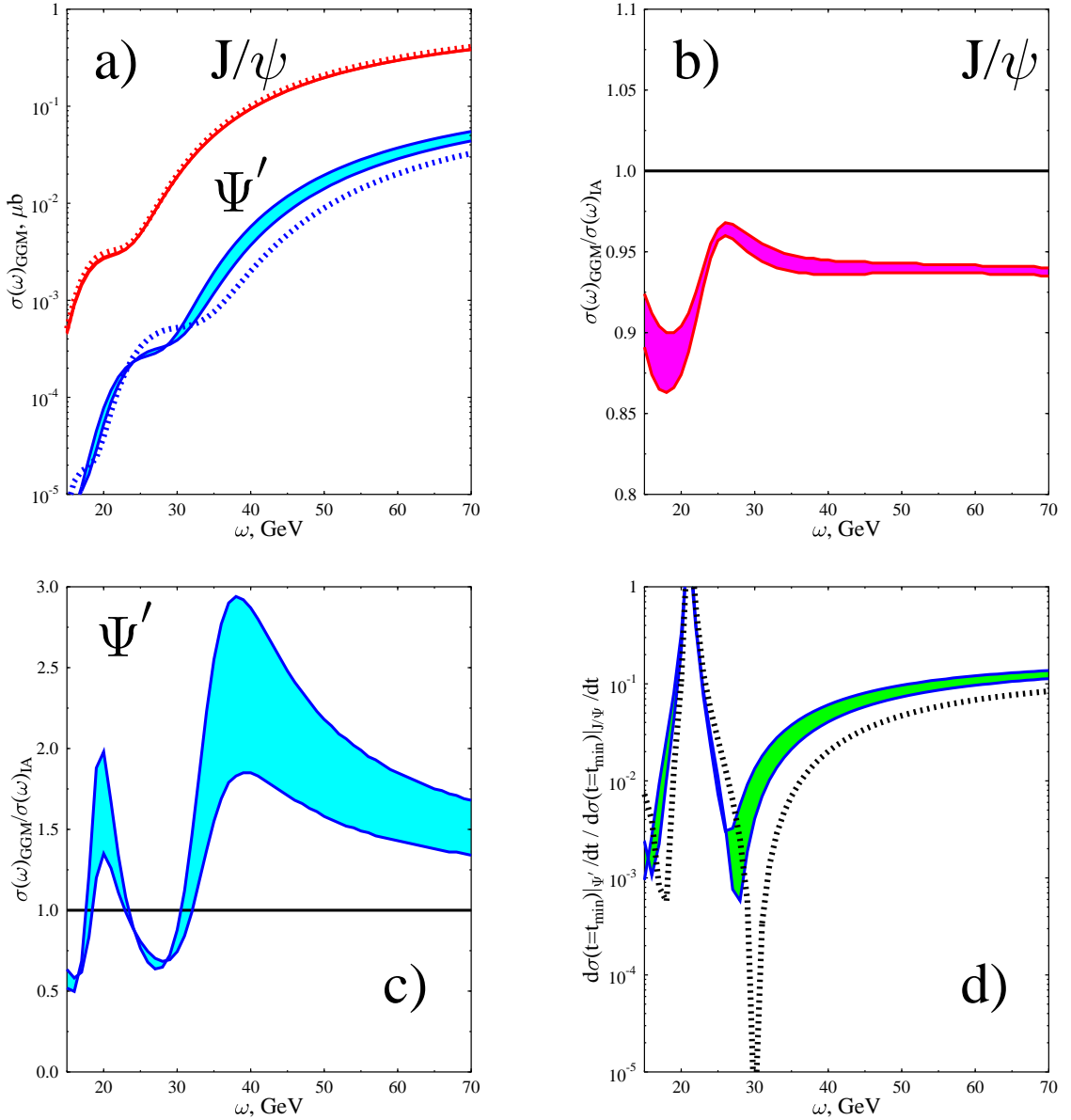


Figure 2: The coherent photoproduction of charmonia off Ca: a). Energy dependence of photoproduction cross sections; b). Ratio of cross sections calculated within the GVDM and IA for  $J/\psi$ ; c). The same for  $\Psi'$ ; d). Ratio of the forward  $\Psi'$ -production cross section to that for  $J/\psi$ . The filled areas show the variation of the cross sections due to the uncertainty of the experimental  $J/\psi N$  cross section.

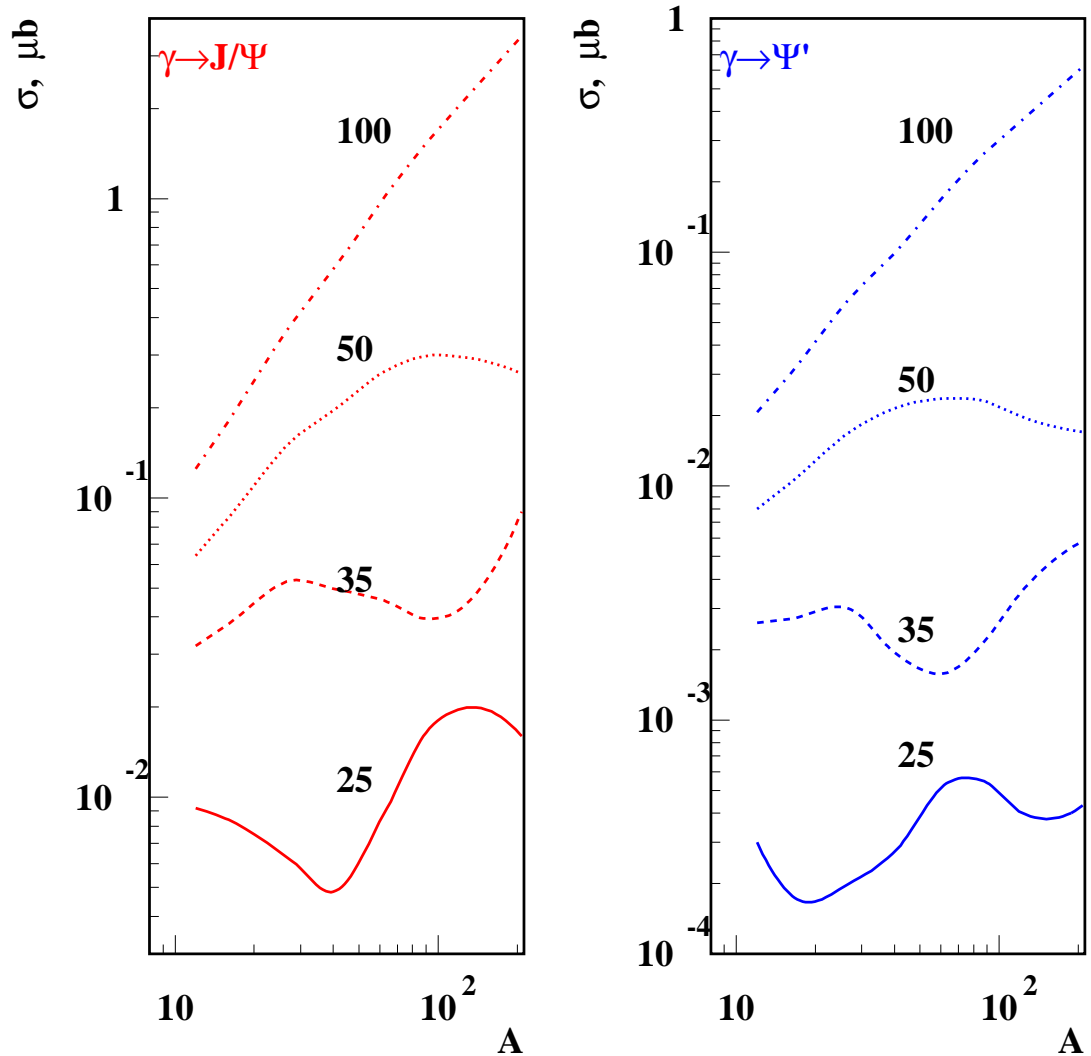


Figure 3: The  $A$ -dependence of the coherent charmonium photoproduction cross sections calculated in the Generalized Vector Dominance Model for different energies of the photon.

is oscillating behavior of the longitudinal nuclear form factor at the relatively large values of  $t_{min}$  in the photoproduction vertex.

The cross section of the  $J/\psi$  photoproduction in the GVDM is close to that calculated in the Impulse Approximation - the shapes of curves are very similar and the values of the cross sections are only slightly reduced at energies below 40 GeV (Fig. 2b). This indicates that it would be very difficult to extract the total  $J/\psi N$  cross section from such a measurement. At the same time, since the nuclear form factor is known with a high precision from the high energy elastic electron-nucleus scattering, one can use the coherent  $J/\psi$  photoproduction off the spherical nuclei to determine the elementary  $\gamma N \rightarrow J/\psi N$  amplitude in a wide range of energies for  $t \sim 0$ .

The picture is qualitatively different for the coherent  $\psi'$  photoproduction off nuclei. Due to the higher threshold  $(E_{th}^{\psi'} - E_{th}^{J/\psi}) \approx 3$  GeV, the direct  $\psi'$  production off nuclei is suppressed in the impulse approximation (for the same incident energy) as compared to the  $J/\psi$  production by the nuclear form factor. Since  $q_{\parallel}^{\gamma\psi'} \approx \frac{m_{\psi'}^2}{m_{J/\psi}^2} q_{\parallel}^{\gamma J/\psi}$ , the minima of the impulse approximation distribution are shifted. The contribution of the nondiagonal term  $\gamma \rightarrow J/\psi \rightarrow \psi'$  essentially increases the  $\psi'$  yield and produces an additional shift of the minima in the spectrum to lower photon energies (Fig. 2c). This results in significant effects, especially, if one analyses the data as a function of the mass number  $A$  at different energies to extract  $A$ -dependence of the  $J/\psi N$  cross sections. It is seen from Fig. 3 that the oscillating form factor significantly influences the  $A$ -dependence that complicates extracting of the genuine  $J/\psi N$  and  $\psi' N$  cross section from such analysis. The oscillation of the cross section with energy can be used to measure in a new way the elementary charmonium photoproduction amplitudes as well as the charmonium-nucleon amplitudes using the coherent charmonium photoproduction off light nuclei [13]. In particular, at the photon energies  $\omega_{\gamma} \approx 0.13 R_A m_{\psi}^2$  (Fig. 2d), the main contribution to the cross section originates from the nondiagonal rescattering. As a result, one can extract from the data the nondiagonal elementary  $J/\psi N \rightarrow \psi' N$  amplitude by measuring the ratio of the  $\psi'$  and  $J/\psi$  yields at zero production angle, because other inputs to this ratio such as the elementary  $\gamma N \rightarrow J/\psi N$  amplitude are fixed from the  $J/\psi$  production. Moreover, since other parameters enter both in the numerator and denominator, the major uncertainties are canceled out. On the other side, the energy dependence of this ratio should originate primarily due to the contribution of the direct  $\psi'$  production. Thus, one would be able to determine the  $\gamma N \rightarrow \psi' N$  amplitude from the measurement of the  $\psi'$ -to- $J/\psi$  ratio. We want to emphasize that the suggested procedure for extracting the nondiagonal amplitude and amplitudes of direct  $J/\psi$  and  $\psi'$  photoproduction from the nuclear measurements is practically model independent.

It is much more difficult to determine the diagonal  $J/\psi N \rightarrow J/\psi N$  and  $\psi' N \rightarrow \psi' N$  amplitudes, which are relevant for the suppression of the charmonium yield in heavy ion collisions.

A naive diagonal VDM with  $\sigma_{tot}(J/\psi N)$  based on the SLAC data [40] leads to a rather significant suppression of the  $J/\psi$  yield:  $\approx 10\% \div 15\%$  for light nuclei, and  $\approx 30\% \div 40\%$  for heavy nuclei. However, we find [12] a strong compensation of the suppression due to the contribution of the nondiagonal transitions. As a result we find that overall the suppression does not exceed  $5\% \div 10\%$  for all nuclei along the periodical table. Hence, an extraction of the diagonal amplitudes from the measured cross sections would require a comparison of high precision data with very accurate theoretical calculations including the nondiagonal transitions. Another strategy is possible if the elementary  $\gamma N \rightarrow J/\psi N$ , and  $\gamma N \rightarrow \psi' N$  photoproduction amplitudes, as well as the nondiagonal amplitude  $J/\psi N \leftrightarrow \psi' N$  would be reliably determined from the medium energy data. In this case it would be possible to determine the imaginary parts of the forward diagonal amplitudes from the GVDM equations (2)

$$\Im f_{J/\psi N \rightarrow J/\psi N} = \frac{f_{J/\psi}}{e} \Im f_{\gamma N \rightarrow J/\psi N} - \frac{f_{J/\psi}}{f_{\psi'}} \Im f_{\psi' N \rightarrow J/\psi N} \quad , \quad (15)$$

$$\Im f_{\psi' N \rightarrow \psi' N} = \frac{f_{\psi'}}{e} \Im f_{\gamma N \rightarrow \psi' N} - \frac{f_{\psi'}}{f_{J/\psi}} \Im f_{J/\psi N \rightarrow \psi' N} \quad . \quad (16)$$

The suggested procedure allows to determine all elementary amplitudes with a reasonable precision from the measurements of  $J/\psi$  and  $\psi'$  photoproduction off the light nucleus at the medium photon energies. The measurement of the coherent charmonium photoproduction off nuclei in this energy region are planned at SLAC [41]. The measurements of coherent production off heavy nuclei and of the quasielastic production with parameters of GVDM fixed from the analysis of light nuclei would provide a critical test of the model.

The main limitation of the suggested procedure is the restriction of the hadronic basis to the two lowest 1S, 2S charmonium states with the photon quantum numbers:  $J/\psi$ ,  $\psi'$ . This is one of the key approximations in the discussed approach. It seems quite reasonable since in the coherent production of vector meson states off nuclei at moderate energies contribution of high mass states is more suppressed by the target form factor. However, we neglected by  $\psi''$  which is nearly degenerate in mass with  $\psi'$ :  $\Delta M = 91$  MeV. The properties of these two states are described well in the charmonium model [42, 43]. In this model  $\psi''$ -meson is described as a  $^3D_1$  state with a small admixture of the  $S$  wave, while  $\psi'$ -meson has a small  $D$ -wave admixture. Namely

$$\begin{aligned} |\psi'\rangle &= \cos \theta |2S\rangle + \sin \theta |1D\rangle, \\ |\psi''\rangle &= \cos \theta |1D\rangle - \sin \theta |2S\rangle. \end{aligned} \quad (17)$$

Since only the  $S$ -wave contributes to the decay of  $\psi$  states into  $e^+e^-$  (at least in the non-relativistic charmonium models) the value  $\theta = 19^\circ \pm 2^\circ$  can be determined from the data on the  $e^+e^-$  decay widths  $\Gamma(\psi' \rightarrow e^+e^-) = 2.19 \pm 0.15$  KeV and the  $\Gamma(\psi'' \rightarrow e^+e^-) = 0.26 \pm 0.04$  KeV. Due to the small difference of masses between the  $\psi'$  and  $\psi''$  mesons the produced  $S$ -wave  $c\bar{c}$ -state does not lose coherence while going through the media at any conceivable energies. The soft interactions cannot transform the  $S$ -state to  $D$ -state with any significant probability. In the soft QCD processes data show that the cross sections of exclusive nondiagonal transitions are negligible for the forward angle scattering. The same conclusion is valid in the PQCD model for the charm dipole-nucleon interactions. Thus, it is more appropriate to use the 1S - 2S basis for description of the propagation of  $c\bar{c}$  through the nucleus. The only resulting change is an increase of  $f_{2S}$  by a factor of  $1/\cos \theta$  as compared to  $f_{\psi'}$  which is within the uncertainties of the model. Since the 2S state ultimately transforms into  $\psi'$  and  $\psi''$  we predict [44]: <sup>2</sup>

$$\frac{\sigma(\psi'')}{\sigma(\psi')} = \tan^2(\theta) \approx 0.1. \quad (18)$$

Influence of the higher mass resonances is expected to be even weaker - the constants  $1/f_V$  relevant for the transition of a photon to a charmonium state  $V$  rapidly decrease with the resonance mass. This is because the radius of a bound state,  $r_V$ , is increasing with the mass of the resonance and therefore the probability of the small size configuration being  $\propto 1/r_V^3$  is decreasing with an increase of mass (for fixed S,L). Besides, the asymptotic freedom in QCD dictates decreasing of the coupling constant relevant for the behavior of the charmonium wave function at small relative distances. Experimentally one finds from the data on the leptonic decay widths that  $1/f_V$  drops by a large factor with increasing mass. An additional suppression arises due to the weakening of the soft exclusive nondiagonal  $VN \leftrightarrow V'N$  amplitudes between states with the different number of nodes. Hence, it seems possible to determine the imaginary parts of diagonal rescattering amplitudes from analysis of the data using the GVDM equations. Since in the medium energy domain the energy dependence of soft rescattering amplitudes is well reproduced by a factor  $s^{0.08}$ , one can determine the real parts of the amplitudes using the Gribov-Migdal relation (Eq. 13).

The above analyses demonstrate that the relative importance of the non-diagonal transitions increases an increase of the quark mass. It would be of interest to investigate experimentally the case of strangeness production. It is likely to correspond to  $\epsilon$  substantially larger than  $\epsilon_\rho \sim 0.2$  but much smaller than  $\epsilon_{J/\psi} \sim 1.7$ .

### 3 Onset of perturbative color opacity at small x and onium coherent photoproduction.

Interaction of small size color singlet objects with hadrons is one of the most actively studied issues in high-energy QCD. The QCD factorization theorem for exclusive meson electroproduction at large  $Q^2$ , and  $J/\psi, \Upsilon$  photoproduction [45, 46] allows to evaluate the amplitude of the production of a vector meson by a longitudinally polarized photon  $\gamma_L + T \rightarrow V + T$  through the convolution of the wave function of the meson

<sup>2</sup>If the s-wave mechanism dominates in the charmonium production in other hard processes the  $\psi''/\psi'$  ratio would be a universal number. Since  $\psi''$  can be easily observed via its characteristic  $D\bar{D}$  decays in a number of the lepton, hadron and nucleus induced processes the study of the discussed process can provide a new way to probing dynamics of charmonium production in various reactions.

at the zero transverse separation, hard interaction block and the generalized (skewed) parton density <sup>3</sup>. The LT approximation differs strongly from the expectations based on Glauber model approaches and on the two gluon exchange models, because it accounts for the dominance of the electroproduction of spatially small quark-gluon wave package and its space-time evolution which leads to formation of a softer gluon field. The latter effect results effectively in an increase of the size of the dipole with increase of the energy.

In perturbative QCD (similar to QED) the total cross section of the interaction of small systems with hadrons is proportional to the area occupied by color within projectile hadron [50] leading to the expectation of the color transparency phenomenon for various hard processes with nuclei. The cross sections of incoherent processes are expected to be proportional to the number of nucleons in the nuclei, while the coherent amplitude is proportional to number of nucleons times the nuclear form factor. Possibility to approximate projectile heavy quarkonium as colorless dipole of heavy quarks can be formally derived from QCD within the limit when mass of heavy quark  $m_Q \rightarrow \infty$  but  $x = 4m_Q^2/s$  is fixed and not extremely small [36]. In this kinematics the size of heavy quarkonium is sufficiently small to justify applicability of PQCD.

For practical purposes the crucial question is at what  $Q^2$  squeezing becomes effective. Probably the most sensitive indicator is the  $t$ -dependence of the meson production. The current HERA data are consistent with the prediction of [46, 36] that the slopes of the  $\rho$  and  $J/\psi$  production amplitudes should converge to the same value. This indicates that at small  $x$  configurations much smaller than average configurations in light mesons ( $d \sim 0.6 \text{ fm}$ ) dominate for  $\rho$ -meson production at  $Q^2 \geq 5 \text{ GeV}^2$ , while the  $J/\psi$  production is dominated by interaction in small size configurations for all  $Q^2$ . Therefore, one expects the regime of color transparency for  $x \geq 0.03$  where the gluon shadowing is very small/absent.

Recently the color transparency (CT) phenomenon was observed at FNAL by E791 experiment [51] which studied the coherent process of dissociation of a 500 GeV pion into two jets off the nuclei. The measurement has confirmed a number of predictions of [49] including the A-dependence, and the transverse and longitudinal momentum distributions of the jets. Previously the color transparency type behavior of the cross section was observed also in the coherent  $J/\psi$  photoproduction at  $\langle E_\gamma \rangle = 120 \text{ GeV}$  [52].

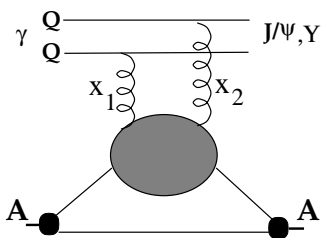
A natural question is whether the color transparency will hold for arbitrary high energies? Two phenomena are expected to work against CT at high energies. One is the LT gluon shadowing. There are theoretical expectations (see discussion below) supported to some extent by the current analyses of the data on DIS scattering off nuclei (which do not extend deep enough into the shadowing region) that the gluon distributions are shadowed in nuclei as compared to the nucleon:  $G_A(x, Q^2)/AG_N(x, Q^2) < 1$ . This obviously should lead to a gradual but calculable in QCD disappearance of color transparency [46, 49], and to onset of a new regime, which we refer to as *the color opacity regime* (one can think of this regime also as a regime of generalized color transparency since a small  $q\bar{q}$  dipole still couples to the gluon field of the target through a two gluon attachment and the amplitude is proportional to the generalized gluon density of the nucleus). Another mechanism for the violation of CT at high energies is the increase of the small dipole-nucleon cross section with energy  $\propto G_N(x, Q^2)$ . For sufficiently large energies this cross section becomes comparable to the meson-nucleon cross sections. One may expect that this would result in a significant suppression of the hard exclusive diffractive processes as compared to the LT approximation. However it seems that this phenomenon is beyond the kinematics achievable for the photoproduction of  $J/\psi$ -mesons in UPC of heavy ions at RHIC ( $x \approx 0.015$ ,  $Q_{\text{eff}}^2 \approx 4 \text{ GeV}^2$ ) but could be important at heavy ion UPC at LHC.

Hence, a systematic study of the onium production in the coherent scattering off nuclei at collider energies will be very interesting. One should emphasize here that with decrease of the size of the onium the eikonal (higher twist) contributions die out quickly (provided  $x$  is kept fixed). In particular, for the  $\Upsilon$  case one probes nuclear gluon fields at the transverse scale of the order of 0.1 fm or  $Q_{\text{eff}}^2 \sim 40 \text{ GeV}^2$ . The  $J/\psi$  case is closer to the border line between the perturbative and nonperturbative domains. As a result the a nonperturbative region appears to give a significant contribution to the production amplitude [53].

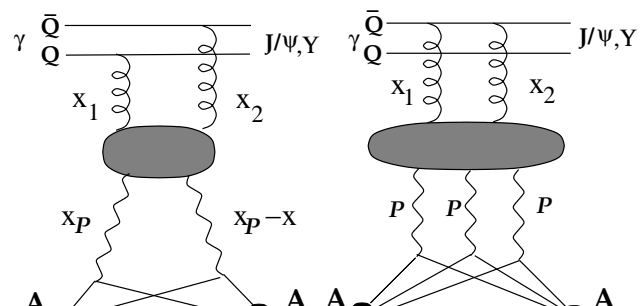
Let us discuss the photoproduction amplitude  $\gamma + A \rightarrow J/\psi(\Upsilon) + A$  in more details. We are interested here in the  $W_{\gamma p}$  range which can be probed at LHC. This region corresponds to rather small values of  $x$ . In this situation interaction of  $q\bar{q}$  pair, which in the final state forms a quarkonium state is still rather far from the BBL. Hence the key problem in the theoretical treatment of the process is taking into account the nuclear shadowing. A number of mechanisms of coherent interactions with several were suggested for

---

<sup>3</sup>Proportionality of the hard diffractive amplitudes to the gluon density of the nucleon was discussed for hard pp diffraction in [47], and for  $J/\psi$  production [48] in the BFKL approximation and for the pion diffraction into two jets [49] in the leading  $\log Q^2$  approximation [49].



(a)



(b)

(c)

Figure 4: Leading twist diagrams for the production of quarkonium off nucleus.

this process. We focus here on the **the leading twist mechanism of shadowing** which is presented by diagrams in Fig.4. There exists qualitative difference between the mechanism of interaction of a small dipole with several nucleons and the case of a similar interaction of an ordinary hadron. Let us for example consider interaction with two nucleons. The leading twist contribution is described by the diagrams where two gluons are attached to the dipole. To ensure that nucleus remains intact in such a process, the color singlet lines should be attached to both nucleons. These diagrams (especially the one of Fig. 4b) are closely related to the diagrams describing the gluon diffractive parton densities (which are measured at HERA), and hence to the similar diagrams for the gluon nuclear shadowing [4].

The amplitude of high energy coherent heavy onium photoproduction is proportional to the generalized gluon density of the target,  $G_T(x_1, x_2, t, Q_{eff}^2)$ , which depends on the light-cone fractions  $x_1$  and  $x_2$  of gluons attached to the quark loop. They satisfy a relation:

$$x_1 - x_2 = \frac{m_V^2}{s} \equiv x \quad (19)$$

If the quark Fermi motion and binding effects were negligible,  $x_2 \ll x_1$ . The resolution scale  $Q_{eff}^2 \geq m_q^2$ , where  $m_q$  is the mass of the heavy quark. Numerical estimates for the photoproduction of  $J/\psi$  give  $Q_{eff}^2 \sim 3-4 \text{ GeV}^2$  [36, 53] reflecting a relatively small mass of c-quark and indicating that this process is on the verge between nonperturbative and perturbative regimes. On the contrary, the mass of the beauty quark is huge on the scale of soft QCD. In this case hard physics dominates, attachments of more than two gluons to  $b\bar{b}$  are negligible and the QCD factorization theorem provides a reliable tool for description of the  $\Upsilon$  production. This is especially true for the ratio of the cross sections of  $\Upsilon$  production from different targets since the higher twist effects due to the overlapping integral of the  $b\bar{b}$  component of the photon and  $\Upsilon$  cancelled out in the ratio. As a result, in the leading twist shadowing approximation the cross section of the process  $\gamma A \rightarrow \Upsilon A$  is proportional to the squared nuclear gluon density distribution and can be written in the form

$$\sigma_{\gamma A \rightarrow VA}(s) = \frac{d\sigma_{\gamma N \rightarrow VN}(s, t_{min})}{dt} \left[ \frac{G_A(x_1, x_2, Q_{eff}^2, t=0)}{AG_N(x_1, x_2, Q_{eff}^2, t=0)} \right]^2 \int_{-\infty}^{t_{min}} dt \left| \int d^2 b dz e^{i\vec{q}_t \cdot \vec{b}} e^{-q_t z} \rho(\vec{b}, z) \right|^2. \quad (20)$$

Numerical estimates using realistic potential model wave functions indicate that for  $J/\psi$ ,  $x_1 \sim 1.5x$ ,  $x_2 \sim x/2$  [53], and for  $\Upsilon$ ,  $x_2/x_1 \sim 0.1$  [56]. Modeling of the generalized parton distributions at moderate  $Q^2$  suggests that to a good approximation  $G(x_1, x_2, t=0)$  can be approximated by the gluon density at  $x = (x_1+x_2)/2$  [46, 54]. For large  $Q^2$  and small  $x$  GPDs are dominated by the evolution from  $x_i(\text{init}) \gg x_i$ . Since the evolution conserves  $x_1 - x_2$ , effect of skewedness is determined primarily by the evolution from nearly diagonal distributions, see Ref. [55] and references therein. In the case of the  $\Upsilon$  production it increases the cross section by a factor  $\sim 2$  [56, 57] and, potentially, this could even obscure the connection of the discussed effect with the shadowing of the nuclear gluon densities. However, the analysis of [58] shows that the ratio of GPD on a nucleus and on a nucleon at  $t=0$  is a weak function of  $x_2$ , slowly dropping from its diagonal value ( $x_2 = x_1$ ) with the decrease of  $x_2$ . Overall this observation is in a agreement with the general trend mentioned above that it is more appropriate to do comparison of diagonal and non-diagonal cases at  $x = (x_1 + x_2)/2$ .

In the case of double scattering contribution (Fig. 4b) there is another way to address the question of the accuracy of the substitution of the ratio of generalized gluon densities by the ratio of diagonal parton densities at the normalization scale. We notice that the amplitude corresponding to Fig. 4b is expressed through the nondiagonal matrix element of the diffractive distribution function,  $\tilde{g}^D(x_{IP}, Q^2, x_1, x, t)$ , which is an analog of generalized parton distribution. In the diagonal limit of  $x_1 = x_2$  it coincides with the diffractive gluon distribution. It depends on the light-cone fraction which nucleon lost in  $|in\rangle$  and  $\langle out|$  states :  $x_{IP}$   $x_{IP} - x$  respectively,  $\beta_{in} = x_1/x_{IP}$ ,  $\beta_{out} = (x_1 - x)/(x_{IP} - x)$ , and  $t, Q^2$ . If we make a natural assumption that

$$\tilde{g}^D(x_1, x, x_{IP}, Q_0^2, t) = \sqrt{g^D(\beta_{in}, Q_0^2, x_{IP}, t)g^D(\beta_{out}, Q_0^2, x_{IP} - x, t)}, \quad (21)$$

we find that numerically in the kinematics we discuss the resulting skewedness effects are small as compared to the uncertainties in the input gluon diagonal diffractive PDFs.

Hence in the following we will approximate the ratio of generalized gluon densities in the nucleus and nucleon by the ratio of the gluon densities in nucleus and nucleon at  $x = m_V^2/s$ . In the case of  $\Upsilon$  use of  $\tilde{x} \sim x/2$  maybe more appropriate. This would lead to slightly larger shadowing effect.

It was demonstrated in [4] that one can express the quark and gluon nuclear shadowing for the interaction with two nucleons in a model independent way through the corresponding diffractive parton densities using the Gribov theory of inelastic shadowing [20] and the QCD factorization theorem for the hard diffraction [59]. An important discovery of HERA is that hard diffraction is indeed dominated by the leading twist contribution and gluons play a very important role in the diffraction (this is loosely referred to as gluon dominance of the Pomeron). Analysis of the HERA diffractive data indicates that in the gluon induced processes probability of the diffraction is much larger than in the quark induced processes [4]. The recent H1 data on diffractive dijet production [60] provide an additional confirmation of this observation. Large probability of diffraction in the gluon induced hard processes could be understood in the s-channel language as formation of color octet dipoles of rather large sizes which can diffractively scatter with a quite large cross section. The strength of this interaction can be quantified using optical theorem and introducing

$$\sigma_{eff}^g = \frac{16\pi}{\sigma_{tot}(x, Q^2)} \frac{d\sigma_{diff}(x, Q^2, t_{min})}{dt} = \frac{16\pi}{(1 + \eta^2)G_N(x, Q^2)} \int_x^0 dx_{IP} g_N^D\left(\frac{x}{x_{IP}}, x_{IP}, Q^2, t_{min}\right), \quad (22)$$

for the hard process of scattering of a virtual photon off the gluon field of the nucleon. Here  $\eta$  is the ratio of the real to imaginary parts of the elementary diffractive amplitude,  $Q^2$  is the momentum scale determining virtuality of the gluons,  $x_{IP}$  is the momentum fraction of the pomeron with the corresponding cut-off scale  $x_{IP}^0 = 0.03$ , and  $g_N^D\left(\frac{x}{x_{IP}}, x_{IP}, Q^2, t_{min}\right)$  is the diffractive gluon density distribution of nucleon which is known from the H1 analysis of the diffractive data at the scale  $Q^2 \approx 4 \text{ GeV}^2$ .

An important feature of this mechanism of coherent interaction is that it is practically absent for  $x \geq 0.02 \div 0.03$  and may rather quickly become important with decrease of  $x$ .

We calculated the ratio of the gluon density distributions in Eq. 20 using the leading twist shadowing model [4] (for the details of calculations see Ref.[61]). As the first step the nuclear gluon density distribution with account of the leading twist shadowing is calculated at the starting evolution scale  $Q_0^2 = 4 \text{ GeV}^2$

$$G_A(x, Q_0^2) = AG_N(x, Q_0^2) - 8\pi\Re\left[\frac{(1-i\eta)^2}{1+\eta^2} \int d^2 b \int_{-\infty}^{\infty} dz_1 \int_{z_1}^{\infty} dz_2 \int_x^{x_{IP}^0} dx_{IP} g_N^D\left(\frac{x}{x_{IP}}, x_{IP}, Q_0^2, t_{min}\right) \rho(\vec{b}, z_1) \rho(\vec{b}, z_2) e^{ix_{IP} m_N(z_1 - z_2)} e^{-\frac{1}{2}\sigma_{eff}(x, Q_0^2)(1-i\eta) \int_{z_1}^{z_2} dz \rho(\vec{b}, z)}\right]. \quad (23)$$

As an input we used the H1 parameterization of  $g_N^D\left(\frac{x}{x_{IP}}, x_{IP}, Q_0^2, t_{min}\right)$ . The effective cross section  $\sigma_{eff}(x, Q_0^2)$  accounts for the elastic rescattering of the produced diffractive state off the nuclear nucleon and is determined by Eq. 22. Numerically it is very large at the starting scale of the evolution, see Fig. 5, and corresponds to the probability of the gluon induced diffraction close to 50%. This indicates that at the initial scale of the evolution interactions in the gluon sector are close to the BBL for  $x \leq 10^{-3}$  for the nucleon case, and even more so for the nuclei, where similar regime should hold for a larger range of the impact parameters.

Note that the double scattering term in Eq. 23 for the nuclear parton densities satisfies QCD evolution, but the higher order terms do not. That is if we use different starting scale of evolution we would obtain different results of  $G(x, Q^2)$ . The reason is that the terms  $\propto \sigma_{eff}^n, n \geq 2$  are sensitive to degree of fluctuations in the cross sections of interaction of diffracting states. These fluctuations increase with increase of  $Q^2$ . This effect is automatically included in the QCD evolution, and it leads to violation of the Glauber - like structure of the expression for the shadowing at  $Q^2 > Q_0^2$ . Approximation for the  $n \geq 3$  rescattering of Eq. 23 corresponds to an assumption that fluctuations are small at  $Q_0^2$  scale since this scale is close enough to the scale of the soft interactions, see discussion in [4]. Thus, at the second step of the calculation we use NLO QCD evolution equations to calculate the shadowing at larger  $Q^2$  using the calculation at  $Q_0^2$  as a boundary condition. In this way we also take into account the contribution of the gluon enhancement at  $x \sim 0.1$  which influences the shadowing at larger  $Q^2$ . Note here that proximity to the BBL in the gluon sector which is reflected in a large value of  $\sigma_{eff}$  may result in corrections to the LT evolution which require further studies.

First we calculate the ratios of the cross sections of coherent photoproduction of  $J/\psi$  and  $\Upsilon$  off nuclei and nucleon (Fig. 6). Such ratios do not depend on the uncertainties of the elementary cross sections and provide

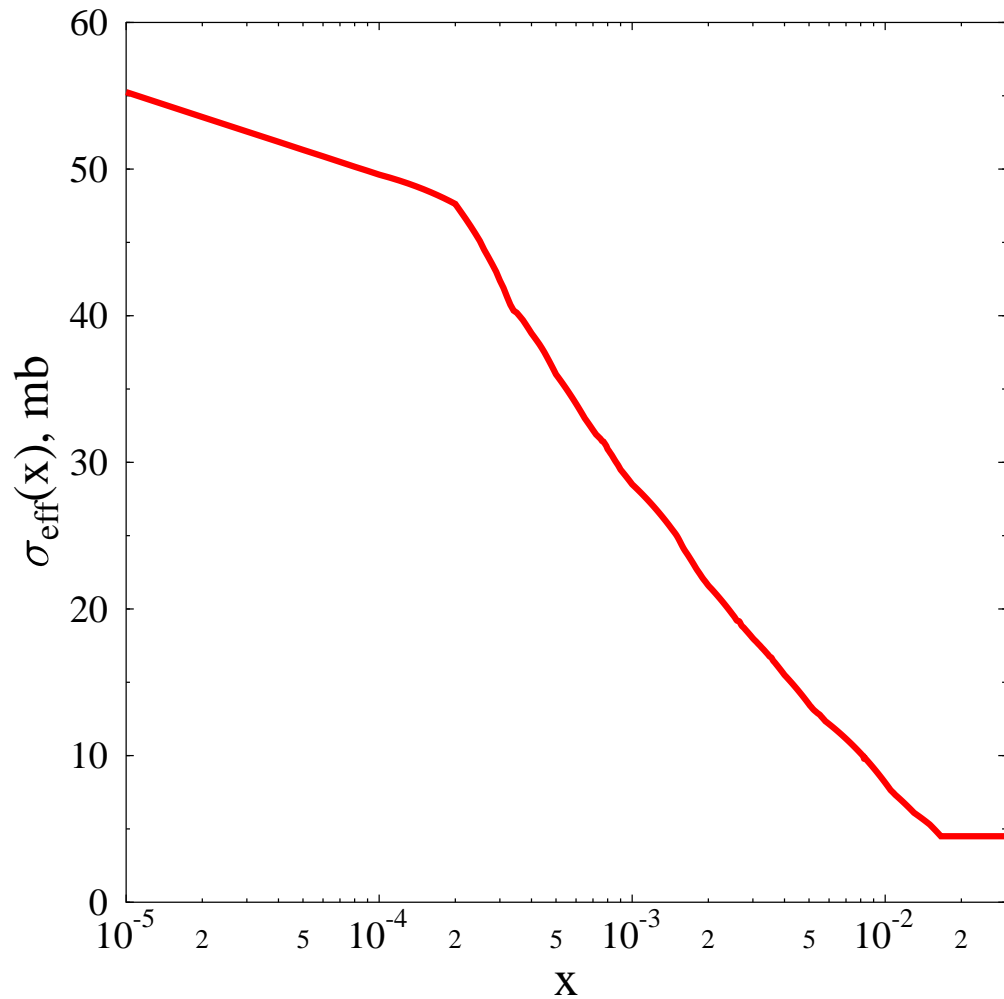


Figure 5: The effective cross section shadowing in the gluon channel,  $\sigma_{eff}(x)$ , at  $Q^2 = 4$  GeV $^2$  as a function of the Bjorken x for H1 parameterizations of the gluon diffractive density.

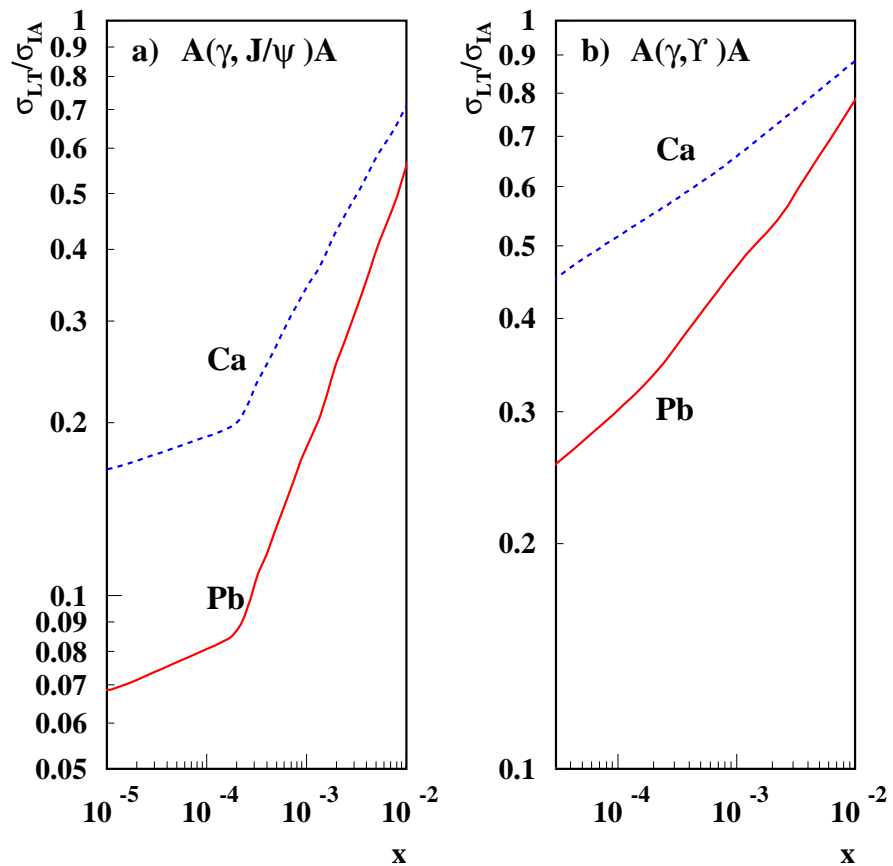


Figure 6: The  $x$ -dependence of the ratio of  $J/\psi$  and  $\Upsilon$  production off Ca and Pb in Glauber model to that in Impulse Approximation(IA). Calculation with the H1 parameterization[60] of the diffractive PDF.

a sensitive test of the role of the LT shadowing effects. In a case of the  $J/\psi$  photoproduction the gluon virtuality scale is 3-4  $GeV^2$  with a significant fraction of the amplitude due to smaller virtualities [36, 53]. Hence we will take the gluon shadowing in the leading twist at  $Q^2 = 4GeV^2$ . Taking a smaller value of  $Q^2$  would result in even larger shadowing effect. In calculations for the  $\Upsilon$  we take  $Q_{eff}^2 = 40GeV^2$ , though the result is not very sensitive to precise value of  $Q_{eff}^2$  since the scaling violation for the gluon shadowing for these  $Q^2$  is rather small. We find that in spite of a small size of  $\Upsilon$ , which essentially precludes higher twist shadowing effects up to very small  $x$ , the perturbative color opacity effect is quite appreciable. It is worth noting that the effective cross section of the rescattering in the eikonal model is determined by the cross section of dipole -nucleon interactions at the distances  $d \sim 0.25 - 0.3fm$  in the  $J/\psi$  case and  $\sim 0.1fm$  in the  $\Upsilon$  case. These cross sections are  $\sim 10 - 15mb$  for  $J/\psi$  and  $\sim 3mb$  for  $\Upsilon$  case for  $x \sim 10^{-4}$  and a factor of 1.5-2 smaller for  $x \sim 10^{-3}$ , see Fig. 13 in Ref. [53]. They are much smaller than the cross sections which enter into calculation of the gluon shadowing in the LT mechanism.

We also estimated the absolute cross section of onium photoproduction for a wide range of the photon energies. This is of interest for the planned measurements of the onium production in the ultraperipheral heavy ion collisions at LHC. The dependence of the momentum-integrated cross sections on the energy  $W_{\gamma N} = \sqrt{s}$  is presented in Fig. 7. In the case of  $J/\psi$  production the calculations are pretty straightforward as the accurate data are available from HERA. The situation is more complicated in the case of the photoproduction of  $\Upsilon$ . So far the information about the elementary  $\gamma + N \rightarrow \Upsilon + N$  cross section is very limited. There is the only ZEUS and H1 data on total cross section for the average energy of  $\sqrt{s} \approx 100GeV$ . Thus, to calculate the forward photoproduction cross section we used a simple parameterization:

$$\frac{d\sigma_{\gamma N \rightarrow VN}(s, t)}{dt} = 10^{-4} B_\Upsilon \left( \frac{s}{s_0} \right)^{0.85} \cdot \exp(B_\Upsilon t), \quad (24)$$

where  $s_0 = 6400$   $GeV^2$ , the slope parameter  $B_\Upsilon = 3.5 GeV^{-2}$  is fixed basing on the analysis of the two gluon form factor in Ref. [62], and the energy dependence follows from the calculations of Ref. [56] of the photoproduction of  $\Upsilon$  in the leading  $\log Q^2$  approximation with an account for the skewedness of the partonic density distributions. This elementary cross section is normalized so that the total cross section is in  $\mu b$ .

## 4 LARGE MASS DIFFRACTION IN THE LEADING TWIST LIMIT

It is well known that inelastic diffraction at small  $t$  gives information on the fluctuations of strength in the projectile-target interactions [29, 63]. Application of this logic to the hadron scattering off nuclei have allowed to explain the A-dependence of two measured diffractive channels in  $pA, \pi A$  scattering assuming that it coincides with the A-dependence of the total cross section of the inelastic diffraction, and the absolute total cross section of  $pA$  diffraction (the data exist for two nuclei only) at the energies 200-400  $GeV$ , see [58] for the review and references. With an increase of energy, the total cross section of  $NN$  interaction increases and fluctuations in the elementary amplitude lead to much smaller fluctuations of the absorption in the scattering off a heavy nuclei. As a result, one can expect much weaker A-dependence of the diffractive cross section [64], in particular,  $\sigma_{diff}(p + A \rightarrow X + A) \propto A^{0.25}$  at LHC energies [1] as compared to  $\sigma_{diff}(p + A \rightarrow X + A) \propto A^{0.7}$  at fixed target energies. For large produced masses we can also understand this suppression using the  $t$  channel picture of the Pomeron exchanges as due to the stronger screening of the triple Pomeron exchange, for review and references see [65].

Diffraction in deep inelastic scattering corresponds to the transition of the (virtual) photon into its hadronic components leaving the nucleus intact. Hence it is similar to elastic hadron-nucleus scattering rather than inelastic diffractive hadron-nucleus scattering.

It was demonstrated recently that in the UPC collisions at LHC it would be possible to study nuclear parton densities using hard charm and beauty production in  $\gamma + A$  interactions [66]. Naturally one can also use these and similar processes to measure diffractive parton densities of nuclei. Since these quantities in the leading twist satisfy the factorization theorem we can analyze them on the basis of the analysis of the diffraction in DIS.

There is a deep connection between shadowing and phenomenon of diffractive scattering off nuclei. The simplest way to investigate this connection is to apply the AGK cutting rules [67]. Several processes con-

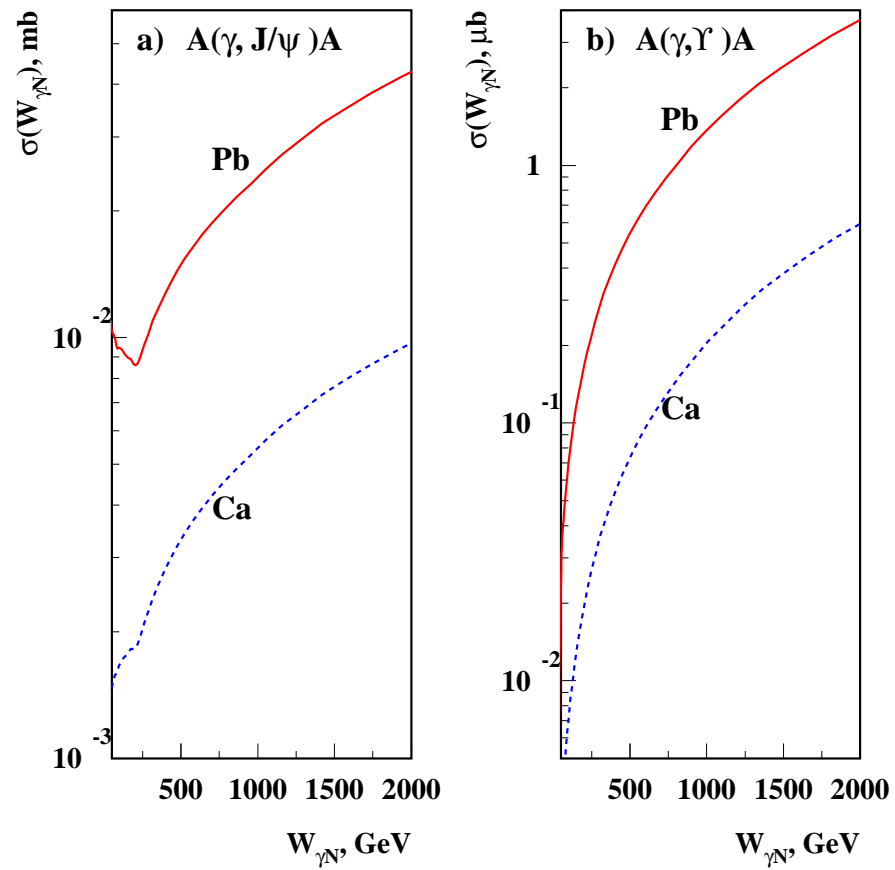


Figure 7: The energy dependence of the coherent  $J/\psi$  and  $\Upsilon$  photoproduction off Ca and Pb in the LT approximation.

tribute to diffraction on nuclei: (i) Coherent diffraction in which the nucleus remains intact, (ii) Break-up of the nucleus without production of hadrons in the nucleus fragmentation region, (iii) Rapidity gap events with hadron production in the nucleus fragmentation region. In Ref. [68] we found that for  $x \leq 3 \cdot 10^{-3}$ ,  $Q^2 \geq 4$  GeV $^2$ , the fraction of the DIS events with rapidity gaps reaches the value of about 30-40% for heavy nuclei, with a fraction of the events of type (iii) rapidly dropping with  $A$ .

We can use the information on  $\sigma_{eff}$  for quarks and gluons to estimate probability of diffraction for different hard triggers at the resolution scale  $\sim Q_0^2$ . First we consider the dependence of the fraction of the events due to coherent diffraction and due to the break-up of the nucleus on the strength of the interaction,  $\sigma_{eff}^j$ , neglecting fluctuations of the interaction strength. We find that for the realistic values of  $\sigma_{eff}^j$  the probability of coherent diffraction is quite large but increases with  $\sigma_{eff}$  very slowly and does not reach the asymptotic value of 1/2 even for very large values of  $\sigma$  (the later feature reflects presence of a significant diffuse edge even in heavy nuclei), see Fig. 8. Thus, it is not sensitive to the fluctuations of  $\sigma_{eff}$ . We also found that the ratio of diffraction with the nucleus break-up and with the nucleus remaining intact is small (10-20%) in a wide range of nuclei, and slowly increasing with increase of  $\sigma_{eff}$ , see Fig. 8. Hence it would require high precision measurements to constrain the dynamics using  $\sigma_{q-el}/\sigma_{tot}$  ratios.

Comparing the values of the fraction of the diffractive events for quark and gluon induced processes off heavy nuclei and proton, we find that the relative importance of the quark induced events is increasing. Therefore, the scaling violation at large  $\beta$  for the diffractive quark distribution in nuclei will be stronger for nuclei than for a proton. Another interesting effect is that for heavy nuclei only genuine elastic components can be produced (inelastic diffraction is zero). Hence, the soft contribution at  $Q_0^2$  due to triple Pomeron exchange is strongly suppressed see e.g. [68]. As a result, nuclear diffractive parton distributions at small  $\beta$  are strongly suppressed (by a factor  $\propto A^{1/3}$ ) at  $Q_0^2$  though this suppression will be less pronounced at large  $Q^2$  due to the QCD evolution. This will lead to breakdown of the universality of the  $\beta$  distributions as a function of  $A$ .

Though the diffractive parton densities change rather slowly with  $Q^2$  leading to a weak variation of the diffractive cross sections with  $Q^2$  (modulus the scaling factor) the fraction of the diffractive events at fixed  $x$  should significantly drop with increase of  $Q^2$  due to a large increase of the inclusive nucleon parton densities and decrease of the nuclear shadowing.

For example, let us consider ultraperipheral collisions (UPC) at LHC where one can measure a the process  $\gamma + A \rightarrow jet_1 + jet_2 + X + A$  in the kinematics where direct photon process  $\gamma + g \rightarrow q\bar{q}$  dominates. In this case if we consider the process at say  $p_t \sim 10$  GeV/c corresponding to  $Q^2 \sim 100$  GeV $^2$  the fraction of diffractive events will be of the order 10%. The background from the strong interaction originates from glancing collisions in which two nucleons interact via a double diffractive process  $pp \rightarrow pp + X$  where  $X$  contains jets. Probability of the hard processes with two gaps is very small at collider energies - even smaller than the probability of the single diffractive hard processes, see e.g. [69]. Therefore, we expect that the background conditions will be at least as good in the diffractive case as in the inclusive case considered in [66]. Thus, it would be pretty straightforward to extract coherent diffraction by simply using anti-coincidence with the forward neutron detector, especially in the case of heavy nuclei, see discussion in [70]. As a result it would be possible to measure in the UPC the nuclear diffractive parton distributions with a high statistical accuracy. It is important that in difference from the diffraction to a vector meson it would be possible to determine on the event by event basis the energy of the photon which induced the reaction, since the rapidity of the photon is close to the rapidity of two jets. As a result it would be possible to perform the measurements for large rapidities (selecting the events generated by a photon of higher of two energies allowed by the kinematics of production particles in the interval of rapidities  $y_1 < y < y_2$ ) and to determine diffractive parton densities for pretty small  $x$ .

## 5 LARGE MASS DIFFRACTION IN THE BLACK BODY LIMIT

One of the striking features of the BBL is the suppression of nondiagonal transitions in the photon interaction with heavy nuclei [17]. Indeed, in the BBL the dominant contribution to the coherent diffraction originates from “a shadow” of the fully absorptive interactions at impact parameters  $b \leq R_A$ , so the orthogonality argument is applicable. We use it to derive the BBL expression for the differential cross section of the

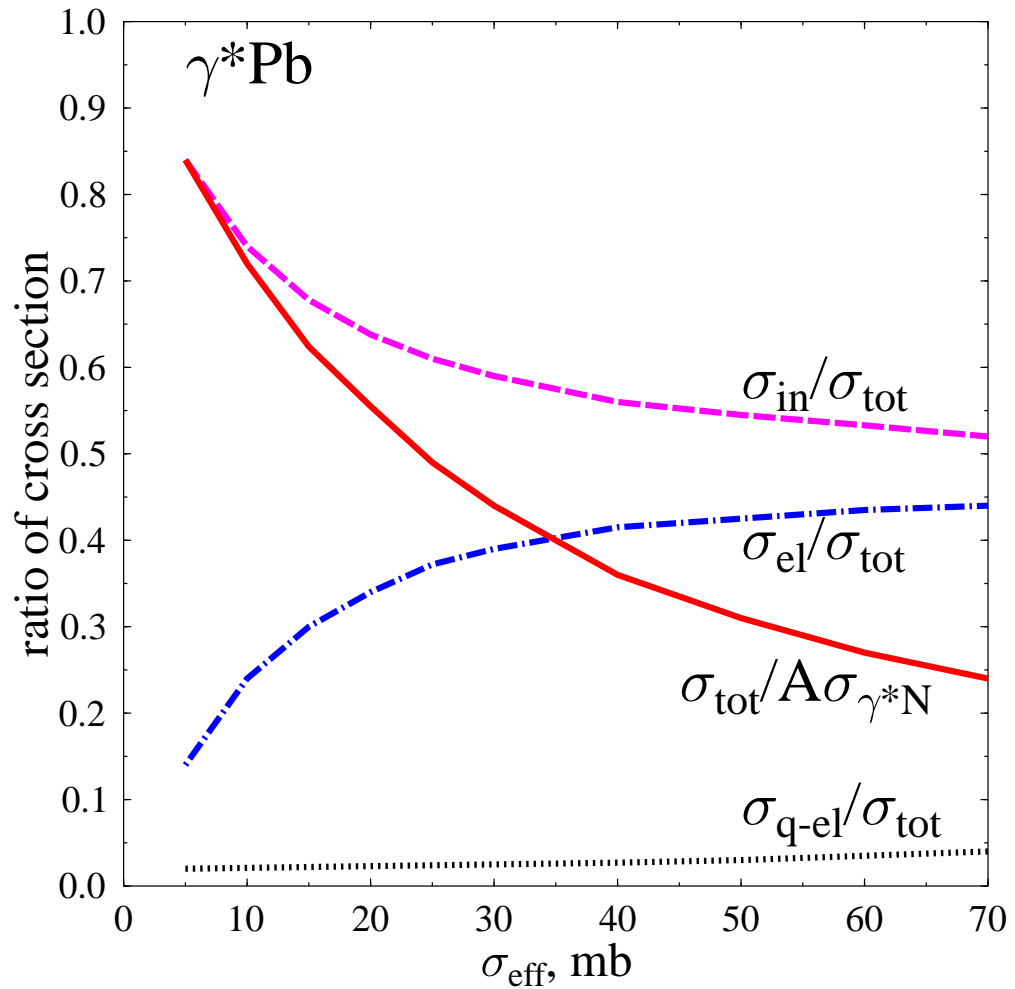


Figure 8: Dependence of the partial cross sections ratios for the hard processes on the effective cross section defined in Eq.21 compared with the shadowing of the inclusive hard process.

production of the invariant mass  $M^2$  for scattering of (virtual) photons [7]. For the real photon case:

$$\frac{d\sigma_{(\gamma+A \rightarrow "M"+A)}}{dt dM^2} = \frac{\alpha_{em}}{3\pi} \frac{(2\pi R_A^2)^2}{16\pi} \frac{\rho(M^2)}{M^2} \frac{4 |J_1(\sqrt{-t}R_A)|^2}{-tR_A^2}. \quad (25)$$

Here  $\rho(M^2) = \sigma(e^+e^- \rightarrow \text{hadrons})/\sigma(e^+e^- \rightarrow \mu^+\mu^-)$ . Comparison of the measured cross section of the diffractive production of states with certain masses with the BBL result (Eq. 25) would allow to determine up to what masses in the photon wave function interaction remains black. Similar equation is valid in the BBL for the production of specific hadronic or quark-gluonic final states ( $q\bar{q}, q\bar{q}g$ , etc) in the case of the coherent nuclear recoil. This allows to measure any component of the light cone photon wave function which interacts with the BBL strength corresponding final states in the coherent processes. The onset of BBL limit for hard processes should reveal itself also in a faster increase with energy of cross sections of photoproduction of excited states as compared to the cross section for the ground state meson. It would be especially advantageous for these studies to use a set of nuclei - one in the medium range, like  $Ca$ , and another with  $A \sim 200$ . This would allow to remove the edge effects and use the length of about 10 fm of nuclear matter.

One especially interesting channel is exclusive diffractive dijet production by real photons. One may expect that for the  $\gamma A$  energies which will be available at EIC or at LHC in UPC the BBL in the scattering off heavy nuclei would be a good approximation for the masses  $M$  in the photon wave function up to few GeV. This is the domain which is described by perturbative QCD for  $x \sim 10^{-3}$  in the case of the proton targets, and larger  $x$  for scattering off nuclei. The condition of large longitudinal distances, a small longitudinal momentum transfer, will be applicable in this case up to quite large values of the produced diffractive mass. In the BBL the dominant channel of diffraction to large masses is production of two jets with the total cross section given by Eq.(25) and with a characteristic angular distribution  $(1 + \cos^2 \theta)$ , where  $\theta$  is the c.m. angle [7]. On the contrary, in the perturbative QCD limit the diffractive dijet production, except the charmed dijet production, is strongly suppressed [71, 72]. The suppression is due to the structure of coupling of the  $q\bar{q}$  component of the real photon wave function to two gluons when calculated in the lowest order in  $\alpha_s$ . As a result, in the real photon case hard diffraction involving light quarks is connected to production of  $q\bar{q}g$  and higher states. Distribution of diffractively produced jets over invariant mass provides an important test of the onset of BBL limit. Really, in the DGLAP/CT regime differential cross section of forward diffractive dijet production should be  $\propto 1/M^8$  and be dominated by charm jet production. This behavior is strikingly different from the BBL limit expressions of [7]. Thus, the dijet photoproduction should be very sensitive to the onset of the BBL regime. We want to draw attention that  $q\bar{q}$  component of the photon light-cone wave function can be measured in three independent diffractive phenomena: in the BBL off the proton, in BBL off a heavy nuclei, in the CT regime where the wave function can be measured as a function of the interquark distance [49]. A competing process for photoproduction of dijets off heavy nuclei is production of dijets in  $\gamma - \gamma$  collisions where the second photon is provided by the Coulomb field of the nucleus. The dijets produced in this process have positive C-parity and hence this amplitude does not interfere with the amplitude of the dijet production in the  $\gamma\gamma$  interaction which have negative C-parity. Our estimates indicate that this process will constitute a very small background over the wide range of energies [9].

## 6 Coherent vector meson production in UPC at LHC

Ultraperipheral collisions(UPC) of relativistic heavy ions at RHIC and LHC open a promising new avenue for experimental studies of the photon induced coherent and incoherent interactions with nuclei at high energies [73, 74]. Really, the LHC heavy ion program [1, 3] will allow studies of photon-proton and photon - nucleus collisions at the energies exceeding by far those available now at HERA for  $\gamma - p$  scattering.

Hence, we can analyze an opportunity to study the phenomena discussed above combining the theory of photo induced processes in the ultraperipheral AA collisions with our studies of the coherent photo(electro) production of vector mesons. We can use the standard Weizsäcker-Williams approximation [75] to calculate the cross section integrated over the momentum of the nucleus which emits the quasireal photons.

The cross section of the vector meson production integrated over the transverse momenta of the nucleus

which emitted a photon can be written in the convoluted form:

$$\frac{d\sigma(AA \rightarrow VAA)}{dy} = N_\gamma(y)\sigma_{\gamma A \rightarrow VA}(y) + N_\gamma(-y)\sigma_{\gamma A \rightarrow VA}(-y). \quad (26)$$

Here  $y$  is the rapidity

$$y = \frac{1}{2} \ln \frac{E_V - p_3^V}{E_V + p_3^V}. \quad (27)$$

The flux of the equivalent photons  $N_\gamma(y)$  is given by a simple expression [73]:

$$N(y) = \frac{Z^2 \alpha}{\pi^2} \int d^2 b \Gamma_{AA}(\vec{b}) \frac{1}{b^2} X^2 \left[ K_1^2(X) + \frac{1}{\gamma} K_0^2(X) \right]. \quad (28)$$

Here  $K_0(X)$  and  $K_1(X)$  are modified Bessel functions with argument  $X = \frac{bm_V e^y}{2\gamma}$ ,  $\gamma$  is Lorentz factor and  $\vec{b}$  is the impact parameter. The Glauber profile factor

$$\Gamma_{AA}(\vec{b}) = \exp \left( -\sigma_{NN} \int_{-\infty}^{\infty} dz \int d^2 b_1 \rho(z, \vec{b}_1) \rho(z, \vec{b} - \vec{b}_1) \right), \quad (29)$$

accounts for the inelastic strong interactions of the nuclei at impact parameters  $b \leq 2R_A$  and, hence, suppresses the corresponding contribution of the vector meson photoproduction.

Recently the STAR collaboration released the first data on the cross section of the coherent  $\rho$ -meson production in gold-gold UPC at  $W_{NN} = \sqrt{s_{NN}} = 130$  GeV [76]. This provides a first opportunity to check the basic features of the theoretical models and main approximations which include the Weizsäcker-Williams (WW) approximation for the spectrum of the equivalent photons, an approximate procedure for removing collisions at small impact parameters where nuclei interact strongly, and the model for the vector meson production in the  $\gamma A$  interactions. In the case of the  $\rho$ -meson production the basic process is understood much better than for other photoproduction processes. Hence, checking the theory for this case is especially important for proving that UPC could be used for learning new information about photon - nucleus interactions. Note here that the inelastic shadowing effects which start to contribute at high energies still remain a few percent correction at energies  $\leq 100$  GeV relevant for the STAR kinematics. For LHC energy range one should account for the blackening of interaction with nuclei. In this case cross section of inelastic diffraction in hadron-nucleus collisions should tend to 0. So major impact for the calculation of the process of diffractive photoproduction of  $\rho$  meson would be necessity to neglect by the contribution of  $\rho'$  [9].

The calculated momentum transfer distributions at the rapidity  $y = 0$  and the momentum transfer integrated rapidity distribution for gold-gold UPC at  $\sqrt{s_{NN}} = 130$  GeV are presented in Figs. 9a,b [10]. Let us briefly comment on our estimate of the incoherent  $\rho$ -meson production cross section. The momentum transfer distribution (dashed line in Fig. 9a) is practically flat in the discussed  $t_\perp$  range. The total incoherent cross section obtained by integration over the wide range of  $t_\perp$  is  $\sigma_{inc} = 120$  mb. To select the coherent production the cut  $t_\perp \leq 0.02$  GeV<sup>2</sup> was used in the data analysis [76]. Correspondingly, the calculated incoherent cross section for this region of  $t_\perp$  is  $\sigma_{inc} = 14$  mb. Our calculations of incoherent production which are based on accounting for only the single elementary diffractive collision obviously present the lower limit. The residual nucleus will be weakly excited and can evaporate only one-two neutrons. The events  $A + A \rightarrow \rho + xn + A_1 + A_2$  were detected by the STAR and identified as a two-stage process - coherent  $\rho$ -production with the subsequent electromagnetic excitation and neutron decay of the colliding nuclei [77]. In particular, the cross section estimated by the STAR for the case when only one of the nuclei is excited and emits several neutrons is  $\sigma_{xn,0n}^\rho = 95 \pm 60 \pm 25$  mb. The momentum transfer distribution for these events is determined by the coherent production. Hence, it differs from that for incoherent events but in the region of very low  $t_\perp$  it is hardly possible to separate them experimentally, and the measured cross section  $\sigma_{xn,0n}^\rho$  includes contribution of incoherent events on the level of 15%.

The total rapidity-integrated cross section of coherent  $\rho$ -meson production calculated in the GVDM for the range of energies available at RHIC is shown in Fig. 10(solid line). We find  $\sigma_{coh}^{th} = 540$  mb at  $\sqrt{s_{NN}} = 130$  GeV. The value  $\sigma_{coh}^{exp} = 370 \pm 170 \pm 80$  mb was obtained at this energy by the STAR from the data analysis at the low momentum transfer  $t_\perp \leq 0.02$  GeV<sup>2</sup>. Thus, before making a comparison we should take into

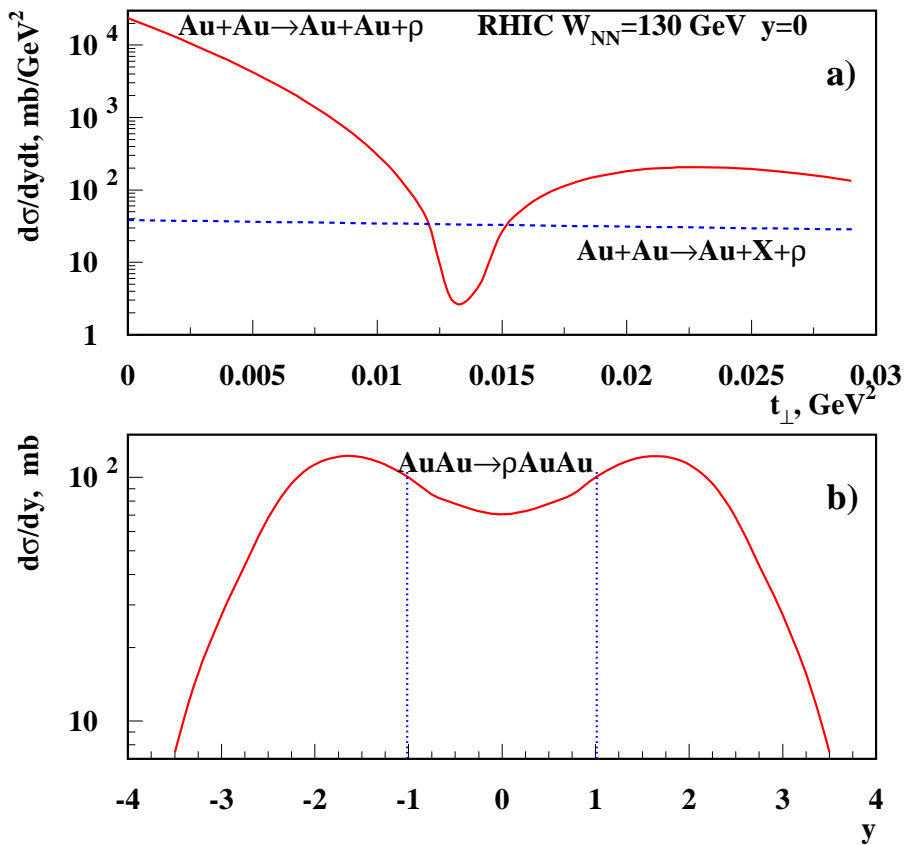


Figure 9: (a) Momentum transfer dependence of the coherent and incoherent  $\rho$ -meson production in Au-Au UPC at  $\sqrt{s_{NN}} = 130$  GeV calculated in GVDM. (b) Rapidity distributions for coherent  $\rho$ -meson production in the gold-gold UPC at  $\sqrt{s_{NN}} = 130$  GeV calculated in GVDM.

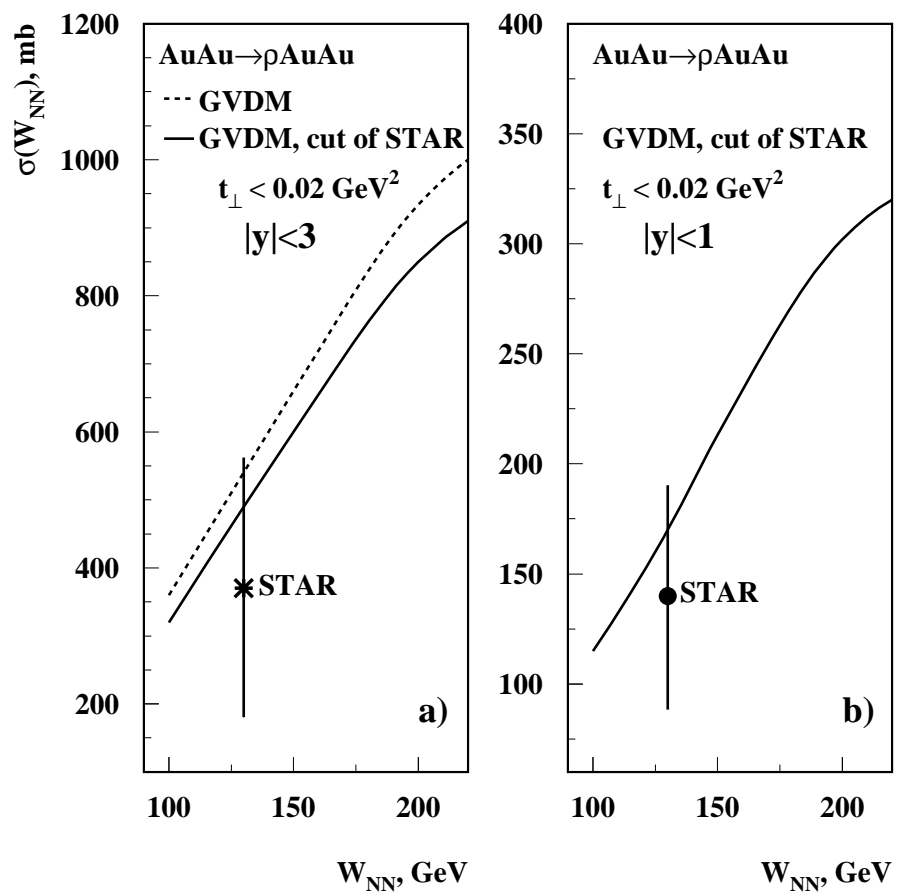


Figure 10: Energy dependence of the total cross section for coherent  $\rho$ -meson production in the gold-gold UPC calculated in the GVDM.

Approximation	Ca-Ca at LHC( $\gamma = 3500$ )	Pb-Pb at LHC( $\gamma = 2700$ )
Impulse	0.6 mb	70 mb
Leading twist	0.2 mb	15 mb

Table 1: Total cross sections of  $J/\psi$  production in UPC at LHC.

account this cut. It leads to a reduction of the cross section by  $\approx 10\%$  (the dashed line in Fig. 10). In our calculations we didn't account for the  $t_\perp$ -dependence of the elementary amplitudes which are rather flat in the considered range of energies and momentum transfers as compared to that for the nucleus form factor. So, in the region of integration important for our analysis it is reasonable to neglect this slope. Nevertheless, an account of this effect would slightly reduce our estimate of the total cross section. Also we neglected a smearing due to the transverse momentum of photons and the interference of the production amplitudes from both nuclei [78].

This latter phenomenon results in the narrow dip in the coherent  $t_\perp$ -distribution at  $t_\perp \leq 5 \cdot 10^{-4}$  GeV $^2$ . All these effects do not influence noticeably the value of the  $t_\perp$ -integrated cross section but can be easily treated and taken into account in a more refined analysis. Thus we find  $\sigma_{coh}^{th} = 490$  mb to be compared to the STAR value  $\sigma_{coh}^{exp} = 370 \pm 170 \pm 80$  mb. Since our calculation does not have any free parameters, this can be considered as a reasonable agreement.

It was suggested in [36, 4] to look for color opacity phenomenon using  $J/\psi$  (photo) electroproduction. This however requires energies much larger than those available at the fixed target facilities and would require use of electron-nucleus colliders. At the same time estimates of the counting rates performed within the framework of the FELIX study [1] have demonstrated that the effective photon luminosities generated in peripheral heavy ion collisions at LHC would lead to significant rates of coherent photoproduction of vector mesons including  $\Upsilon$  in reaction

$$A + A \rightarrow A + A + V. \quad (30)$$

As a result it would be possible to study at LHC photoproduction of vector mesons in Pb-Pb and Ca-Ca collisions at energies much higher than the range  $W_{\gamma p} \leq 17.3$  GeV covered at the fixed target experiment at FNAL [52]. Note that even current experiments at RHIC ( $W_{\gamma p} \leq 25$  GeV) should also exceed this limit. As it is clearly indicated by the STAR study the coherent photoproduction, leaving the both interacting nuclei intact, can be reliably identified by using the veto triggering from the two-side Zero Degree Calorimeters which select the events not comprising the escaped neutrons. The additional requirement which enables to remove contribution of the incoherent events with the residual nucleus in the ground state is selection of the produced quarkonium with small transverse momentum. In Fig. 11 we compare the momentum transfer distributions for the coherent  $J/\psi$  and  $\Upsilon$  photoproduction calculated in the Leading Twist shadowing model with the corresponding distributions for incoherent photoproduction. Note that we estimated the upper limit of incoherent cross section simply as the free elementary cross section on the nucleon target multiplied by the number of nucleons  $A$ .

In Fig. 12a,b we present the rapidity distributions of the  $J/\psi$  coherent production for peripheral collisions at LHC calculated including effects of gluon shadowing and in the impulse approximation. At the central rapidities we find suppression by a factor 4 for a case of Ca and more strong, by a factor 6 for Pb. The total cross sections are given in Table 1. The rapidity distributions for coherent  $\Upsilon$  production in the UPC with Ca and Pb beams are shown in Fig. 12c,d and the corresponding total cross sections are given in Table 2. As it is seen from comparison of the Leading Twist shadowing based calculations to that performed in the Impulse Approximation the yield of  $\Upsilon$  is expected to be suppressed by a factor 2 at central rapidities due to the leading twist nuclear shadowing.

Hence, study of the coherent photoproduction of the heavy quarkonium states at LHC opens an important

Approximation	Ca-Ca at LHC( $\gamma = 3500$ )	Pb-Pb at LHC( $\gamma = 2700$ )
Impulse	1.8 $\mu b$	133 $\mu b$
Leading twist	1.2 $\mu b$	78 $\mu b$

Table 2: Total cross sections of  $\Upsilon$  production in UPC at LHC.

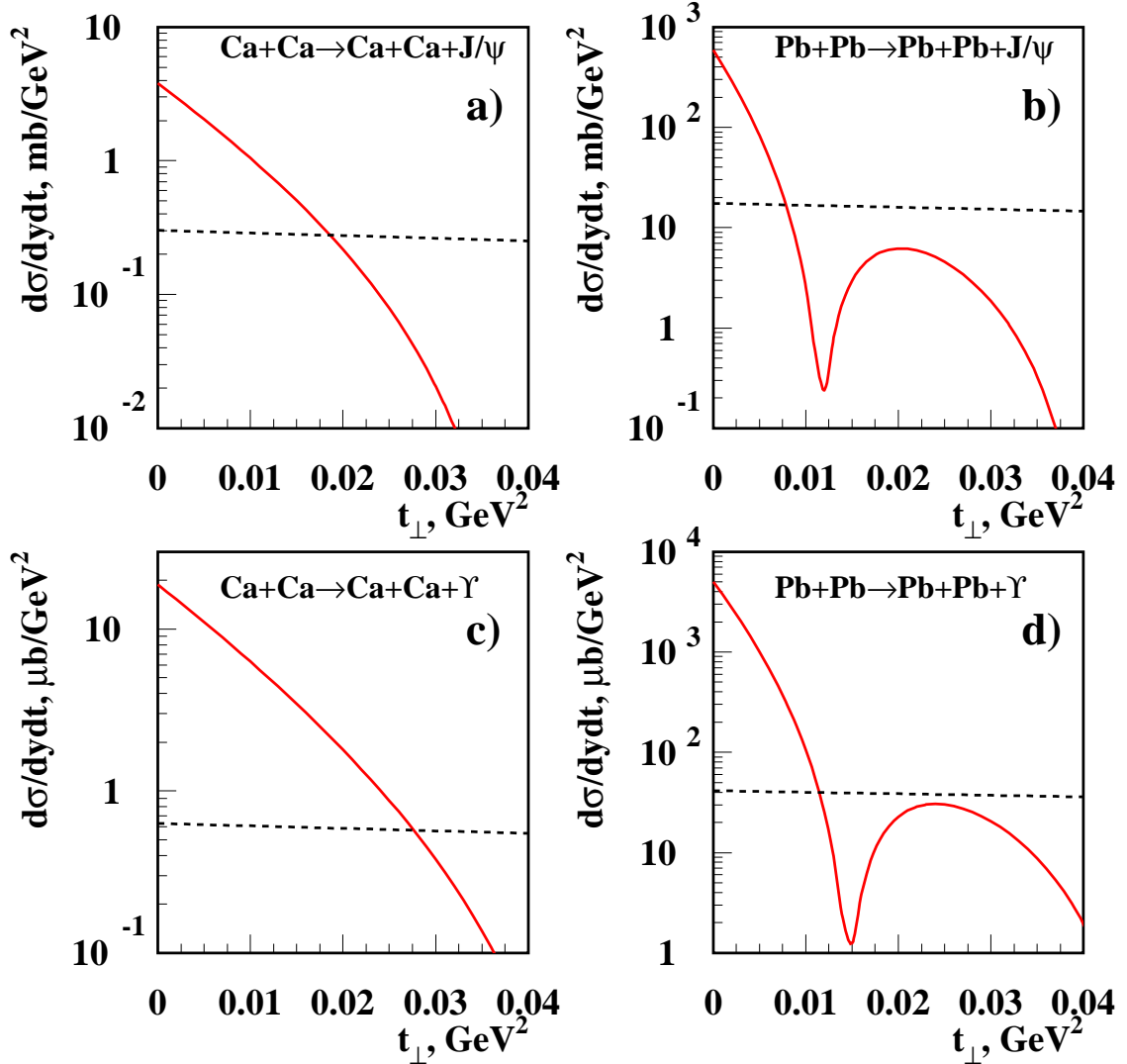


Figure 11: The momentum transfer distribution for the coherent  $J/\psi$  and  $\Upsilon$  production in Ca-Ca and Pb-Pb in UPC at LHC. Solid line - calculation with the Leading twist shadowing, dashed line - the momentum transfer distribution for the incoherent photoproduction.

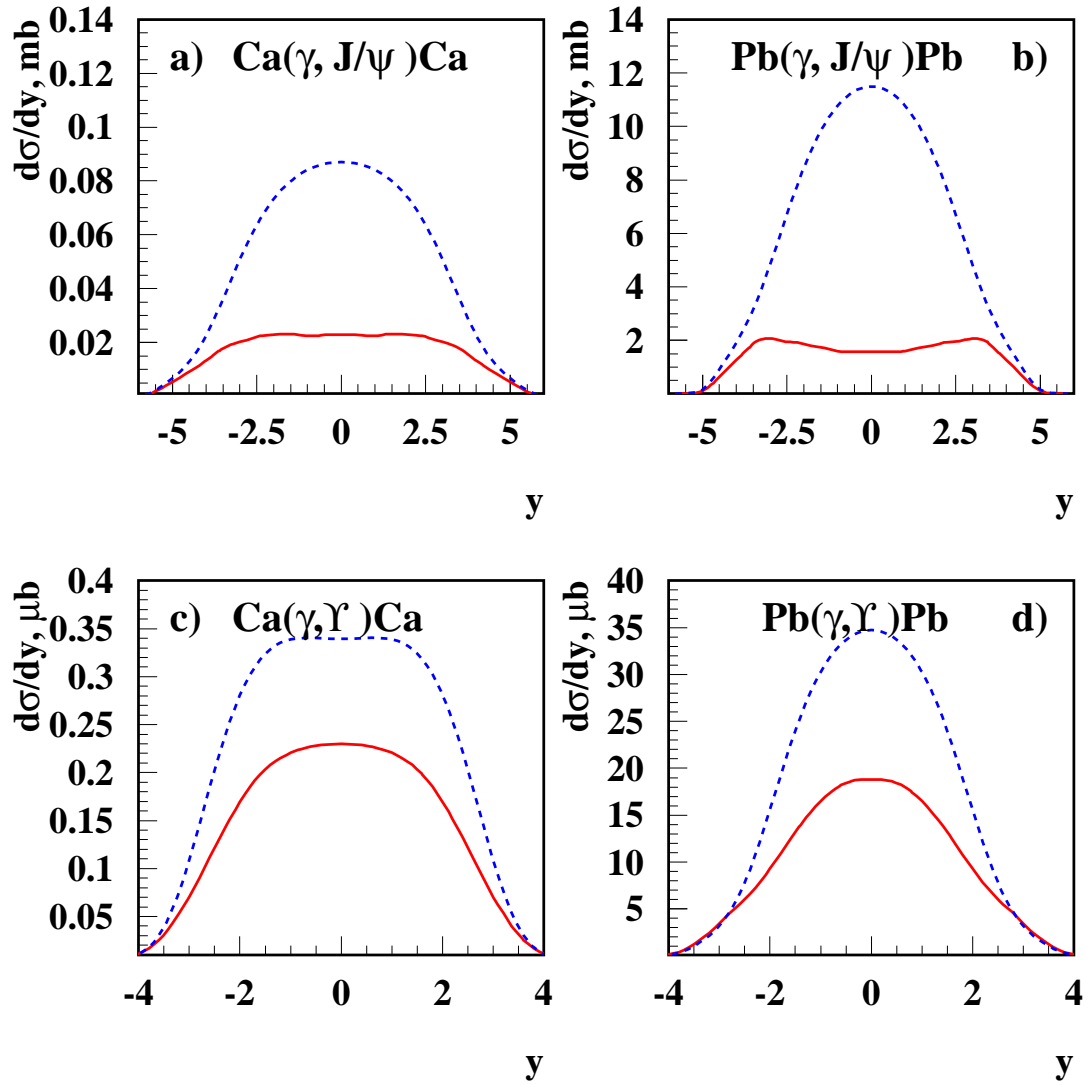


Figure 12: The rapidity distributions for the  $J/\psi$  and  $\Upsilon$  coherent production off Ca and Pb in UPC at LHC calculated with the leading twist shadowing based on H1 parameterization of gluon density(solid line) and in the Impulse Approximation(dashed line)

avenue for investigating the nuclear gluon distributions and the shadowing effects in the kinematics which would be very hard to probe in any other experiments.

## 7 CONCLUSIONS

We demonstrated that coherent diffraction off nuclei provides an effective method of probing a possible onset of BBL regime in hard processes at small  $x$ . We predict a significant increase of the ratio of the yields of  $\rho, \rho'$  mesons in coherent processes off heavy nuclei due to the blackening of the soft QCD interactions in which fluctuations of the interaction strength are present. An account of nondiagonal transitions leads to a prediction of a significant enhancement of production of heavier diffractive states especially production of high  $p_t$  dijets. Study of these channels may allow to get an important information on the onset of the black body limit in the diffraction of real photons. We argued that the fluctuations of strengths of interactions has been observed at intermediate energies in the diffractive photoproduction of vector mesons. We discuss the opportunity to look for the transition from the nuclear color transparency to the regime of the color opacity in the ultrarelativistic peripheral ion collisions at LHC.

We thank J.Bjorken, A.Mueller, G.Shaw, members of the UPC study group, and our coauthors M.McDermott, A.Freund, V.Guzey, L.Gerland, for useful discussions and GIF and DOE for support. M.S. and M.Z. thank INT for hospitality while this work was completed.

## References

- [1] FELIX Collaboration (E. Lippmaa et al.). CERN-LHCC-97-45, LHCC-I10; A. Ageev *et al.*, J. Phys. G **28**, R117 (2002).
- [2] G. Baur, K. Hencken, D. Trautmann, S. Sadovsky and Y. Kharlov, Phys. Rept. **364**, 359 (2002); [arXiv:hep-ph/0112211].
- [3] S. Beole *et al.* [ALICE Collaboration], CERN-LHCC-98-19
- [4] L. Frankfurt and M. Strikman, Eur. Phys. J. A **5**, 293 (1999).
- [5] L.McLerran and R.Venugopalan, Phys.Rev. **D50**, 225 (1994); Phys.Rev. **D59**, 094002 (1999).
- [6] A. H. Mueller, Nucl. Phys. B **307**, 34 (1988).  
Y. V. Kovchegov, Phys. Rev. D **55**, 5445 (1997); [arXiv:hep-ph/9701229].
- [7] L. Frankfurt, V. Guzey, M. McDermott and M. Strikman, Phys. Rev. Lett. **87**, 192301 (2001); [arXiv:hep-ph/0104154].
- [8] L. Frankfurt, M. Strikman and M. Zhalov, Phys. Lett. B **540**, 220 (2002); [arXiv:hep-ph/0111221].
- [9] L. Frankfurt, M. Strikman and M. Zhalov, Phys. Lett. B **537**, 51 (2002).
- [10] L. Frankfurt, M. Strikman and M. Zhalov, Phys. Rev. **C67**, 034901 (2003); [arXiv:hep-ph/0210303].
- [11] L. Frankfurt, M. Strikman and M. Zhalov, Nucl. Phys. **A711**, 243 (2002).
- [12] L. Frankfurt, L. Gerland, M. Strikman and M. Zhalov, [arXiv:hep-ph/0301028].
- [13] L. Frankfurt, L. Gerland, M. Strikman and M. Zhalov, [arXiv:hep-ph/0301077].

- [14] L. Frankfurt, V. Guzey, M. Strikman and M. Zhalov, [arXiv:hep-ph/0304218]
- [15] R. J. Glauber, *Boulder Lectures in Theoretical Physics*, vol.1, (Interscience Publ. Inc. , NY)(1959);  
K. Gottfried and D. R. Yennie, *Phys. Rev.* **182**, 1595 (1969)  
Erratum-*ibid. D* **2**, 2737 (1970);  
G. V. Bochmann, *Phys. Rev. D*6, 1938 (1972).
- [16] T. H. Bauer, R. D. Spital, D. R. Yennie and F. M. Pipkin, *Rev. Mod. Phys.* **50**, 261 (1978); [Erratum-*ibid. 51*, 407 (1978)].
- [17] V. N. Gribov, *Zh. Eksp. Teor. Fiz.* **57**, 1306 (1969).
- [18] S. J. Brodsky and J. Pumplin, *Phys. Rev.* **182**, 1794 (1969).
- [19] A. Donnachie and G. Shaw, in *Electromagnetic Interactions of Hadrons*, edited by A. Donnachie and G. Shaw (Plenum, New York, 1978), Vol. 2, pp. 164-194;  
H. Fraas, B. Read, and D. Schildknecht, *Nucl. Phys.* **B86** , 346 (1975);  
P. Ditsas and G. Shaw, *Nucl. Phys. B* **113**, 246 (1976).
- [20] V. N. Gribov, *Sov. J. Nucl. Phys.* **9**, 369 (1969);  
*Sov. Phys. JETP* **29**, 483 (1969);  
*Sov. Phys. JETP* **30**, 709 (1970).
- [21] L. L. Frankfurt and M. Strikman, *Phys. Rep.* **160**, 235 (1988).
- [22] L. Frankfurt, V. Guzey and M. Strikman, *Phys. Rev. D* **58**, 094039 (1998).
- [23] M. Beiner, H. Flocard, N. Van Giai, P. Quentin, *Nucl. Phys.* **A238**, 29 (1975).
- [24] S. L. Belostotsky et al., *Proceedings of the conference Modern developments in nuclear physics*, Novosibirsk 1987, World Scientific, 1988, p. 191.
- [25] L. Lapikas, G. van der Steenhoven, L. Frankfurt, M. Strikman and M. Zhalov, *Phys. Rev. C* **61**, 064325 (2000); [arXiv:nucl-ex/9905009];  
L. Frankfurt, M. Strikman and M. Zhalov, *Phys. Lett. B* **503**, 73 (2001); [arXiv:hep-ph/0011088].
- [26] A. Pautz and G. Shaw, *Phys. Rev. C* **57**, 2648 (1998).
- [27] H. Alvensleben et al., *Nucl. Phys.* **B18**, 333 (1970);  
G. McClellan et al., *Phys. Rev. D* **4**, 2683 (1971).
- [28] A. Donnachie and P. V. Landshoff, *Phys. Lett. B* **478**, 146 (2000); [arXiv:hep-ph/9912312].
- [29] M. Good and W. Walker, *Phys. Rev. D* **120**, 1857 (1960).
- [30] B. Badelek, M. Krawczyk, K. Charchula and J. Kwiecinski, *Rev. Mod. Phys.* **64** (1992) 927.
- [31] H. Abramowicz and A. Caldwell, *Rev. Mod. Phys.* **71**, 1275 (1999); [arXiv:hep-ex/9903037].
- [32] L. Frankfurt, V. Guzey, M. McDermott and M. Strikman, *JHEP* **0202**, 027 (2002); [arXiv:hep-ph/0201230].
- [33] U. Camerini et al., *Phys. Rev. Lett.* **35**, 483 (1975).

- [34] L. Frankfurt and M. Strikman, *Prog. Part. Nucl. Phys.* **27**, 135 (1991).
- [35] J. Hufner, B. Kopeliovich, *Phys. Lett.* **B426**, 154 (1988).
- [36] L. Frankfurt, W. Koepf and M. Strikman, *Phys. Rev. D* **54**, 3194 (1996), *ibid* **57**, 512 (1998).
- [37] K. Suzuki, A. Hayashigaki, K. Itakura, J. Alam and T. Hatsuda, *Phys. Rev. D* **62**, 031501 (2000); [arXiv:hep-ph/0005250].
- [38] R. Vogt, *Phys. Rept.* **310**, 197 (1999);  
C. Gerschel, J. Hufner, *Annu. Rev. Nuc. Part. Sci.* **49**, 255 (1999).
- [39] D. Kharzeev and H. Satz, In R.C. HWA (ed.): *Quark-gluon plasma*, vol.2, 395-453 and [arXiv:hep-ph/9505345].
- [40] R.L. Anderson et al., *Phys. Rev. Lett.* **38**, 263 (1977).
- [41] V. Ghazikhanian et al. SLAC-Proposal E-160, 2000.
- [42] E. Eichten, K. Gottfried, T. Kinoshita, J. B. Kogut, K. D. Lane and T. M. Yan, *Phys. Rev. Lett.* **34**, 369 (1975); [Erratum-*ibid.* **36**, 1276 (1976)].
- [43] J. M. Richard, *Z. Phys. C* **4** (1980), 211 (1980).
- [44] L. Frankfurt, L. Gerland, M. Strikman and M. Zhalov, [arXiv:hep-ph/0302009].
- [45] J. C. Collins, L. Frankfurt and M. Strikman, *Phys. Rev. D* **56**, 2982 (1997); [arXiv:hep-ph/9611433].
- [46] S. J. Brodsky, L. Frankfurt, J. F. Gunion, A. H. Mueller and M. Strikman, *Phys. Rev. D* **50**, 3134 (1994); [arXiv:hep-ph/9402283].
- [47] L. Frankfurt and M. Strikman, *Phys. Rev. Lett.* **63**, 1914 (1989); [Erratum-*ibid.* **64**, 815 (1990)].
- [48] M. G. Ryskin, *Z. Phys. C* **57**, 89 (1993).
- [49] L. Frankfurt, G. A. Miller and M. Strikman, *Phys. Lett. B* **304**, 1 (1993).
- [50] F. E. Low, *Phys. Rev. D* **12**, 163 (1975).
- [51] E. M. Aitala *et al.* [E791 Collaboration], *Phys. Rev. Lett.* **86**, 4773 (2001).
- [52] M. D. Sokoloff *et al.*, *Phys. Rev. Lett.* **57**, 3003 (1986).
- [53] L. Frankfurt, M. McDermott and M. Strikman, *JHEP* **0103**, 045 (2001); [arXiv:hep-ph/0009086].
- [54] A. V. Radyushkin, In “At the Frontier of Particle Physics / Handbook of QCD”, edited by M. Shifman (World Scientific, Singapore, 2001), vol. 2\* p. 1037-1099; [arXiv:hep-ph/0101225].
- [55] A. Freund and M. McDermott, *Phys. Rev. D* **65**, 074008 (2002).
- [56] L. L. Frankfurt, M. F. McDermott and M. Strikman, *JHEP* **9902**, 002 (1999); [arXiv:hep-ph/9812316].
- [57] A. D. Martin, M. G. Ryskin and T. Teubner, *Phys. Lett. B* **454**, 339 (1999); [arXiv:hep-ph/9901420].

- [58] L. Frankfurt, V. Guzey and M. Strikman, J. Phys. G **27**, R23 (2001);  
[arXiv:hep-ph/0010248].
- [59] J. C. Collins, Phys. Rev. D **57**, 3051 (1998); [Erratum-ibid. D **61**, 019902 (1998)];  
[arXiv:hep-ph/9709499].
- [60] C. Adloff *et al.* [H1 Collaboration], Eur. Phys. J. C **20**, 29 (2001).
- [61] L. Frankfurt, V. Guzey and M. Strikman, preprint hep-ph/0303022.
- [62] L. Frankfurt and M. Strikman, Phys. Rev. D **66**, 031502 (2002);  
[arXiv:hep-ph/0205223].
- [63] E. L. Feinberg and I. Ia. Pomeranchuk, Suppl. Nuovo Cimento **III**, 562 (1956).
- [64] L. Frankfurt, G. A. Miller and M. Strikman, Phys. Rev. Lett. **71**, 2859 (1993);  
[arXiv:hep-ph/9309285].
- [65] A. B. Kaidalov, V. A. Khoze, A. D. Martin and M. G. Ryskin, [arXiv:hep-ph/0303111].
- [66] S. R. Klein, J. Nystrand and R. Vogt, Phys. Rev. C **66**, 044906 (2002);  
[arXiv:hep-ph/0206220].
- [67] V.A. Abramovskii, V.N. Gribov and O.V. Kancheli, Yad. Fiz. **18**, 595 (1973).
- [68] L. Frankfurt and M. Strikman, Phys. Lett. **B382**, 6 (1996).
- [69] K. Goulianos [CDF Collaboration], Acta Phys. Polon. B **33** (2002) 3467 [arXiv:hep-ph/0205217].
- [70] M. Strikman, M. G. Tverskoy and M. B. Zhalov, Phys. Lett. **B459**, 37 (1999);  
[arXiv:nucl-th/9806099].
- [71] S. J. Brodsky and J. Gillespie, Phys. Rev. **173**, 1011 (1968).
- [72] M. Diehl, Z. Phys. C **66**, 181 (1995).
- [73] G. Baur, K. Hencken, D. Trautmann, S. Typel and H. H. Wolter, Prog. Part. Nucl. Phys. **46**, 99 (2001);  
[arXiv:nucl-th/0011061].
- [74] S. Klein, J. Nystrand, Phys. Rev. C **60**, 014903 (1999);  
[arXiv:hep-ph/9902259].
- [75] E. Fermi, Z. Physik, **29**, 315 (1924);  
C. F. von Weizsacker, Z. Physik, **88**, 612 (1934);  
E. J. Williams Phys. Rev., **45**, 729 (1934).
- [76] C. Adler *et al.* [STAR Collaboration], Phys. Rev. Lett. **89**, 272302 (2002);  
[arXiv:nucl-ex/0206004].
- [77] A. J. Baltz, S. R. Klein and J. Nystrand, Phys. Rev. Lett. **89**, 012301 (2002);  
[arXiv:nucl-th/0205031].
- [78] S. R. Klein, J. Nystrand, Phys. Rev. Lett. **84**, 2330 (2000).